Preoperative Evaluation of Invasive and Noninvasive Intraductal Papillary-Mucinous Neoplasms of the Pancreas

Clinical, Radiological, and Pathological Analysis of 123 Cases

Satoshi Nara, MD, Hiroaki Onaya, MD, PhD,† Nobuyoshi Hiraoka, MD, PhD,‡ Kazuaki Shimada, MD, PhD,* Tsuyoshi Sano, MD, PhD,§ Yoshihiro Sakamoto, MD, PhD,* Minoru Esaki, MD, PhD,* and Tomoo Kosuge, MD, PhD**

Objective: We aimed to investigate preoperative findings that are useful to distinguish intraductal papillary-mucinous neoplasm (IPMN) subtypes.

Methods: One hundred twenty-three patients who underwent pancreatectomy for IPMN were analyzed clinicopathologically and radiologically. Invasive IPM carcinomas (IPMCs) were subdivided into early-stage nonaggressive (minimally invasive IPMC [MI-IPMC]) and more advanced and aggressive (invasive carcinoma originating in IPMC [IC-IPMC]) subtypes according to our recently proposed pathological criteria.

Results: The lesions consisted of 27 IPMNs with low-grade dysplasia, 14 IPMNs with moderate dysplasia, 21 IPMNs with high-grade dysplasia, 30 MI-IPMCs, and 31 IC-IPMCs. Multidetector-row computed tomography detected a component of invasive carcinoma in IC-IPMC with 86% sensitivity and 100% specificity. In patients with IPMNs other than IC-IPMC, multivariate analysis demonstrated 3 significant predictive factors of malignancy: IPMN size (>40 mm), IPMN duct type (main pancreatic duct or mixed type), and the presence of a mural nodule or thick septum. The diagnostic score obtained using these 3 factors showed a strong correlation with the presence of malignancy.

Conclusions: For preoperative evaluation of patients with IPMN, it is recommended to rule out IC-IPMC using multidetector-row computed tomography and then to categorize IPMN other than IC-IPMC according to malignant potential based on the diagnostic score.

Key Words: intraductal papillary-mucinous neoplasm, pancreas, minimal invasion, diagnostic score, prognostic factor

(*Pancreas* 2009;38: 8–16)

Intraductal papillary-mucinous neoplasm (IPMN) of the pancreas is a well-characterized entity both clinically and pathologically. IPMNs are characterized by intraductal proliferation of neoplastic mucinous cells, which usually form papillae and lead to cystic dilation of the pancreatic ducts, forming a clinically and macroscopically detectable mass.[1,2] IPMNs include a wide spectrum of tumors that vary in their malignant potential. It is highly speculated that IPMN progresses from low-grade, moderate, and high-grade dysplasia (carcinoma in situ [CIS]) to invasive IPM carcinoma (IPMC) and eventually to invasive adenocarcinoma.[1–5] Depending on the grade of IPMN during the progression from noninvasive IPMN to invasive IPMC, the choice of treatment varies from a conservative approach to radical pancreatectomy with lymph node (LN) dissection.[6] Therefore, it is very important to determine the subtype of IPMN accurately before surgery to optimize the therapy.

Preoperative distinction of IPMN subtypes is not easy, even when multiple modalities are used.[7] It is necessary to inspect the entire lesion because various tumor grades are usually present in 1 lesion; however, this is problematic to perform directly and biopsy of the lesion is difficult because IPMNs are located in the pancreas and often shows cystic features. Some groups reported the high accuracy of pancreas juice cytology[8] or peroral intraductal pancreatoscopy,[9] but these procedures require expertise and are not free from complications; thus, routine practice of these modalities remains limited.

Previous studies have proposed some factors that are predictive of IPMN malignancy, such as the presence of symptoms (particularly jaundice), positive pancreatic juice cytology, tumor size greater than 30 to 50 mm, main pancreatic duct (MPD) type or mixed type, dilatation of MPD, the presence of a mural nodule, papillary projection, a thick septum, and wall thickening.[7,8,10–12] Except for the former two, these features can be observed by radiological examination, but these factors are not always related to the malignancy, and none of them can be used alone.

Another problem is that no unequivocal pathological criteria for distinguishing invasive IPMC have been established. The recent consensus is that the malignant potential of IPMN is dependent on the presence of invasive cancer and its extent.[13–19] However, invasive IPMC categorized by the Armed Forces Institute of Pathology (AFIP) and World Health Organization classifications[1,2] covers cancer with variable biological behavior, with the 5-year survival rate varying substantially between 24% and 60%.[13–19] Therefore, invasive IPMC should be regarded separately as either aggressive or nonaggressive. The classification of the Japan Pancreas Society subdivides invasive IPMC into minimally invasive IPMC (MI-IPMC) and invasive carcinoma originating in IPMC (IC-IPMC) (Fig. 1).[20] Minimally invasive IPMC represents invasive IPMC with early-stage nonaggressive characteristics, whereas IC-IPMC represents a more advanced tumor. Minimally invasive IPMC has been reported to have a better surgical outcome than IC-IPMC,[21,22] although the criteria used for defining MI-IPMC are still unclear.[20] Recently, we

From the *Hepatobiliary and Pancreatic Surgery Division and †Diagnostic Radiology Division, National Cancer Center Hospital; and ‡Pathology Division, National Cancer Center Research Institute, Tokyo; and §Hepatobiliary and Pancreatic Surgery Division, Aichi Cancer Center Hospital, Nagoya, Japan.

Received December 3, 2007.
Accepted for publication May 15, 2008.

Reprints: Satoshi Nara, MD, Hepatobiliary and Pancreatic Surgery Division, National Cancer Center Hospital, 5-1-1 Tsukiji, Chuo-ku, Tokyo 104-0045, Japan (e-mail: sanara@ncc.go.jp).

The authors have no direct or indirect commercial or financial incentives associated with publishing this article.

This work was supported by a Grant-in-Aid for Third Term Comprehensive 10-Year Strategy for Cancer Control from the Ministry of Health, Labor and Welfare of Japan and a Grant-in-Aid for Scientific Research from the Ministry of Education, Culture, Sports, Science and Technology of Japan.

ISSN: 0885-3177
DOI: 10.1097/MPA.0b013e318181b90d

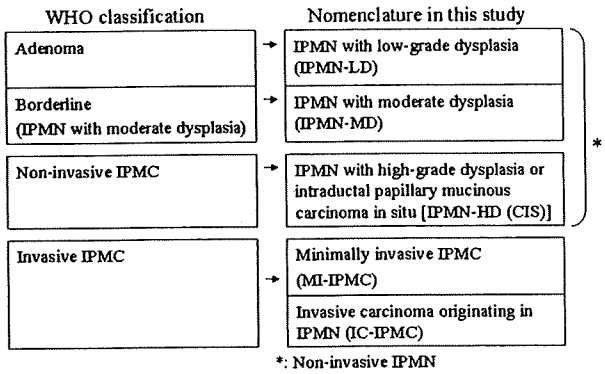

FIGURE 1. The nomenclature of IPMN used in this study is based on AFIP classification[1] and corresponded to the World Health Organization classification.[2] Invasive IPMCs are further divided into MI-IPMC and IC-IPMC according to our diagnostic criteria,[23] which is based on the classification of the Japan Pancreas Society.[20]

proposed simple and practical diagnostic criteria for MI-IPMC[23] and used them to classify IPMN in 104 patients. Those with MI-IPMC showed a good outcome similar to that of noninvasive IPMN after curative resection, whereas patients with IC-IPMC showed a worse outcome similar to that of conventional ductal carcinoma of the pancreas. In addition, IC-IPMCs were frequently associated with LN metastasis, necessitating LN dissection during operation, whereas no LN metastasis was observed among patients with MI-IPMCs.[22,23] Thus, precise discrimination between MI-IPMC and IC-IPMC is important not only for predicting the postoperative outcome, but also for deciding the operative procedure.

In the present retrospective study, we examined 123 patients with IPMN and assessed their clinical and radiological findings for preoperative prediction of IPMN pathological subtypes.

MATERIALS AND METHODS

Study Population

This study was approved by the ethics committee of the National Cancer Center, Japan. Between January 1984 and December 2006, a total of 123 patients underwent pancreatectomy for IPMN at the National Cancer Center Hospital, Japan. Seventy-eight (63%) of the surgical operations were performed after January 2001. Eight patients who also had ductal carcinoma of the pancreas that was not directly associated with IPMN were excluded from the study. The study patients are composed of 70 men and 53 women aged 40 to 84 years (mean, 64.7 years). Upon pathological examination, 5 patients were found to have multiple IPMNs in the resected specimen. We chose 1 lesion with the highest grade, then the largest lesion among multiple IPMNs, and used it for this study. Clinical data and characteristics of the IPMNs are summarized in Table 1. Every patient was followed up in the outpatient clinic every 1 to 3 months during the first postoperative year, and every 6 to 12 months thereafter. No patient was lost to follow-up. Clinical and laboratory data for every patient were obtained from the medical records.

Pathological Examination

All of the IPMNs were pathologically reexamined, and the diagnosis of IPMN was confirmed. Surgically resected specimens were fixed in 10% formalin and cut into serial 5-mm-thick slices, horizontally in the pancreas head and sagittally in the

TABLE 1. Demography of Patients With IPMNs

Pathological Diagnosis	IPMN-LD or IPMN-MD (n = 41)	IPMN-HD (CIS) (n = 21)	MI-IPMC (n = 30)	IC-IPMC (n = 31)	Total (n = 123)	*P*
Mean age, yrs	64.1 ± 8.0	62.0 ± 9.6	64.9 ± 8.6	67.4 ± 10.4	64.7 ± 9.1	0.186
Median age (range), yrs	65 (42–77)	60 (40–80)	66 (41–76)	69 (45–84)	66 (40–84)	
Male, %	25 (61.0%)	10 (47.6%)	19 (63.3%)	16 (51.6%)	70 (56.9%)	0.599
Chief complaints						0.024*
Complaints (−)	27	13	15	12	67	
Complaints (+)	14	8	15	19	56	
Radiological findings						
Tumor location						0.005
Ph included	29	15	22	12	78	
Ph excluded	12	6	8	15	41	
Total pancreas (diffuse)	0	0	0	4	4	
rIPMN size, mm	35.7 ± 16.2	44.5 ± 17.4	53.6 ± 31.6	48.4 ± 30.1	44.8 ± 25.4 (10–136)	0.022
rMPD diameter, mm	4.5 ± 2.8	6.5 ± 4.8	10.7 ± 6.6	6.4 ± 4.5	6.9 ± 5.2 (1–31)	<0.001
rIPMN type						<0.001
rMPD type	0	5	11	10	26	
rBD type	33	12	6	8	59	
rMixed type	8	4	13	13	38	
Mural nodule (>3 mm), %	10 (24%)	15 (71%)	20 (67%)	15 (48%)	60 (49%)	<0.001
Thick septum (>2 mm), %	11 (27%)	8 (38%)	14 (47%)	13 (42%)	46 (37%)	0.343
Size of invasive cancer, mm	—	—	<5	36.1 ± 17.7 (6–90)	—	

*Comparison between noninvasive IPMN and invasive IPMN (MI-IPMC + IC-IPMC) by χ^2 test.

Ph indicates pancreas head; rIPMN size, IPMN size measured on CT; rIPMN type, IPMN type determined based on CT findings.

pancreas body and tail. All the sections were stained with hematoxylin and eosin for pathological examination. After histopathological examination of all the sections, the lesion was classified as IPMN with low-grade dysplasia (IPMN-LD), moderate dysplasia (IPMN-MD), high-grade dysplasia (IPMN-HD; CIS), or invasive IPMC according to the AFIP classification.[1] The lesion was graded by the highest degree of atypia. Invasive IPMCs were further divided into MI-IPMC or IC-IPMC according to our proposed criteria.[23] We classified the invasive features of IPMC into 3 patterns: infiltrative growth, mucous rupture, and expansive growth. *Infiltrative growth* is an invasive pattern commonly seen in conventional ductal carcinoma of the pancreas, showing tubular or mucinous invasion. On the other hand, mucous rupture and expansive growth are unique features of IPMC, which grows expansively with large amounts of mucus secretion. *Mucous rupture* refers to mucous lakes around an intraductal IPMC, sometimes containing scanty floating cancer cells, formed by rupture of pancreatic ducts through intraductal high pressure. *Expansive growth* refers to the loss of the basement membrane because of marked dilatation of pancreatic duct, sometimes resulting in the involvement (erosion or fistula formation) of the bowel wall or major vessels. We defined *minimal invasion* as (*a*) an infiltrative growth of 5 mm or less, (*b*) mucous rupture not associated with infiltrative growth of more than 5 mm, or (*c*) expansive growth without fistula formation with major vessels. And when at least 1 feature beyond the previously mentioned criteria of minimal invasion was present, the lesion was diagnosed as IC-IPMC. Invasive carcinoma originating in IPMC was originally defined as a lesion consisting of IPMN and invasive carcinoma with predominance of the IPMN component.[20] This type of invasive carcinoma shows continuous transition between invasive carcinoma and intraductal IPMC. In this study, we also included a new group in which invasive carcinoma apparently originated from IPMN but was predominant over the IPMN component because there was no statistically significant survival difference between IC-IPMCs with predominant IPMN component and IC-IPMCs with predominant invasive cancer component in our preliminary analysis.

The measured size of an IPMN (excluding the invasive component) was denoted as the *pIPMN size*, defined as the maximum diameter of microscopically recognized noninvasive IPMN. The size of invasive cancer was measured separately in patients with MI-IPMC and IC-IPMC. The duct type of IPMN was also determined according to where the IPMN was mainly present. When the IPMN was located mainly in the MPD and extended to a small region of the branch duct (BD) (length, <1 cm), it was defined as the MPD type. When the IPMN located mainly in the BD and extended to a small region of the

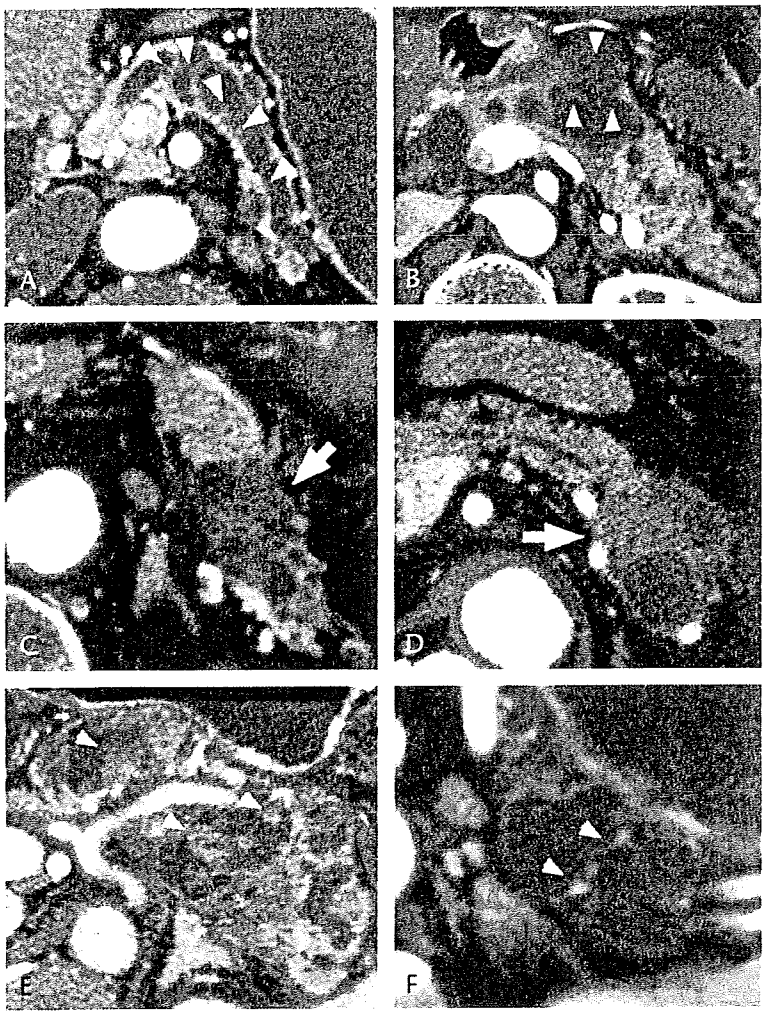

FIGURE 2. A and B, MDCT images show papillary projections in the dilated pancreatic ducts (arrowheads). Papillary projections appear as subtle brushlike low attenuations along the wall of the pancreatic ducts, reflecting the extent of IPMN. C and D, MDCT images of IC-IPMCs. The invasive cancer components (arrows) are depicted as areas of low attenuation adjacent to or surrounding the cystic IPMN lesions. The retropancreatic invasion adjacent to the splenic artery is shown (arrow) (D). E and F, MDCT images showing mural nodules (E) and thick septa (F). E, Various-sized mural nodules are evident in the intraductal carcinoma component (arrowheads). F, The thick septum is indicated by arrowheads in noninvasive IPMCs.

MPD (length, <1 cm), it was defined as the BD type; otherwise, the IPMN was defined as the mixed type.

Radiological Examination

All 123 patients underwent contrast-enhanced computed tomography (CT) and extracorporeal ultrasonography (US) examinations, whereas magnetic resonance cholangiopancreatography (MRCP) was performed in 77 patients (63%). As endoscopic retrograde cholangiopancreatography and endoscopic US are not routinely performed at our institution, data for both examinations were excluded from the present analysis. The CT images were obtained using single-slice helical CT machines before 2000, and thereafter using multidetector-row CT (MDCT) with a 1- to 2-mm section thickness. Of the 123 patients, 71 (58%) underwent MDCT examinations.

The CT images were retrospectively reviewed independently by 2 investigators (S.N. and H.O.) without knowledge of the pathological diagnosis. Discrepancy was less than 5%, and cases with disagreement were resolved by discussion. The size of the IPMN (designated as rIPMN size), the duct type

TABLE 2. Univariate Analysis of Preoperative (Clinical or Radiological) Findings Associated With Subtypes of IPMNs

Variables	(1) IPMN-LD or IPMN-MD (n = 41)	(2) IPMN-HD (CIS) (n = 21)	(3) MI-IPMC (n = 30)	(4) IC-IPMC (n = 31)	Total (n = 123)	P (χ^2 or Fisher Exact Test) (2) (3) vs (4)	(1) vs (2) (3)	(2) vs (3)
Sex						0.643	0.690	0.265
Male	25	10	19	16	70			
Female	16	11	11	15	53			
Age, yrs						0.020	0.858	0.969
≤70	32	16	23	16	87			
>70	9	5	7	15	36			
Chief complaint						0.155	0.287	0.400
(−)	27	13	15	12	67			
(+)	14	8	15	19	56			
Jaundice						0.098	0.500	0.506
(−)	41	21	28	26	116			
(+)	0	0	2	5	7			
CEA, ng/mL						0.288	0.376	0.134
≤10	40	21	26	26	113			
>10	1	0	4	5	10			
CA-19-9, U/mL						<0.001	0.296	0.119
≤37	31	20	23	10	84			
>37	10	1	7	21	39			
Radiological findings								
Detection of invasive cancer on CT*						<0.001	0.126	0.134
(−)	41	21	26	6	94			
(+)	0	0	4	25	29			
Tumor location						0.055	0.847	0.881
Ph included	29	15	22	16	82			
Ph excluded	12	6	8	15	41			
Tumor distribution						0.110	0.532	0.034
1 segment	35	20	21	20	96			
2 or 3 segments	6	1	9	11	27			
rIPMN size, mm						0.321	<0.001	0.917
≤40	31	8	11	15	65			
>40	10	13	19	16	58			
rMPD diameter, mm						0.120	0.005	0.020
≤8	36	17	14	24	91			
>8	5	4	16	7	32			
rIPMN duct type						0.371	<0.001	0.006
rMPD or rMixed	8	9	24	23	64			
rBD	33	12	6	8	59			
Mural nodule (>3 mm) or thick septum (>2 mm)						0.079	0.001	0.969
(−)	24	5	7	13	49			
(+)	17	16	23	18	74			

*CT images obtained using both single-slice helical CT and MDCT.
CEA indicates carcinoembryonic antigen; Ph, pancreas head.

of IPMN (designated as rIPMN duct type, and MPD, BD, and mixed type being denoted as rMPD, rBD, and rMixed type, respectively), the distribution of IPMN (head/uncus, body, or tail), and the MPD diameter (designated as rMPD diameter) were determined. The *rIPMN size* was defined as the maximum diameter of an entire noninvasive IPMN lesion, including not only the definitely cystic and/or intraductal papillary component, but also subtle papillary projections reflecting spread along the pancreatic duct (Figs. 2A, B).[24] The invasive component was excluded from the measurement of rIPMN size. The size of invasive component was measured separately depending on the CT findings. The presence of invasive carcinoma in patients with IC-IPMC was regarded as positive when an irregularly shaped hypoattenuating solid mass was detected adjacent to or surrounding an IPMN on contrast-enhanced CT.[25] The replacement of the pancreatic parenchyma by a hypoattenuating solid mass, proliferation into the extrapancreatic tissue, and encasement of surrounding vessels were all regarded as signs of invasion, similarly to the conventional invasive ductal carcinoma of the pancreas (Figs. 2C, D). We also assessed the presence of a mural nodule (if its size was >3 mm; Fig. 2E)[10] or a thick septum (if its size was >2 mm; Fig. 2F)[12] on image analysis including CT, US, and MRCP, if available.

Statistical Analysis

Continuous data were presented as mean ± SD. The cutoff values for rIPMN and pIPMN size for differentiating benign and malignant lesions were investigated by constructing receiver operating characteristic (ROC) curves. Differences between categorical variables were evaluated using χ^2 test or Fisher exact test. One-way analysis of variance was used to compare the means of 3 or more groups. Significant predictors in the univariate analysis were included in a backward stepwise logistic regression model for multivariate analysis. Differences at $P < 0.05$ were considered statistically significant. Statistical analyses were performed using SPSS 11.0J software (SPSS Inc, Chicago, Ill).

RESULTS

Postoperative pathological examination revealed that the studied lesions are composed of 27 IPMN-LDs, 14 IPMN-MDs, 21 IPMN-HD (CIS), 30 MI-IPMCs, and 31 IC-IPMCs (Table 1). More than half of the IPMNs were discovered incidentally in asymptomatic patients during health check-up or follow-up examinations after treatment of other organ diseases, and such cases were significantly common among noninvasive IPMNs ($P = 0.024$; Table 1). Chief complaints at the initial presentation included abdominal pain (n = 28), exacerbation of diabetes mellitus (n = 9), back pain (n = 7), jaundice (n = 7), weight loss (n = 7), appetite loss (n = 4), general fatigue (n = 2), carbohydrate antigen 19-9 (CA-19-9) elevation (n = 2), vomiting (n = 1), and fever (n = 1).

TABLE 4. Accuracy of CT Detection of Invasive Cancer in IC-IPMC

A. MDCT

	CT detection of invasive cancer		Sensitivity 86%
Pathological diagnosis	(+)	(−)	Specificity 100%
IC-IPMC (+)	18	3	21
IC-IPMC (−)	0	50	50
	18	53	71

B. Single-slice helical CT

	CT detection of invasive cancer		Sensitivity 70%
Pathological diagnosis	(+)	(−)	Specificity 90%
IC-IPMC (+)	7	3	10
IC-IPMC (−)	4	38	42
	11	41	52

Preoperative Detection of IC-IPMC

To test which preoperative (clinical and radiological) variables were closely associated with IPMN pathological subtypes, their relationship was examined (Table 2). As reported previously,[21–23,26] the postoperative outcome of patients with IC-IPMC was significantly worse than that of patients with MI-IPMC or noninvasive IPMN, and LN metastasis was exclusively associated with IC-IPMC, underlining the importance of preoperative detection of IC-IPMC for therapeutic planning. Univariate analysis showed that the following preoperative variables were closely associated with the pathological subtypes of IC-IPMC: older than 70 years, the presence of invasive cancer detected on CT (both single-slice helical CT and MDCT), and CA-19-9 greater than 37 U/mL (Table 2). Multivariate analysis showed

TABLE 3. Multivariate Analysis of Preoperative (Clinical or Radiological) Findings Associated With Subtypes of IPMNs

	Odds Ratio (95% CI)	P*
IPMN-HD (CIS) and MI-IPMC vs IC-IPMC		
Invasive cancer detected on CT†	53.9 (14.0–208)	<0.001
CA-19-9 >37 U/mL	4.38 (1.22–15.8)	0.0024
IPMN-LD or IPMN-MD vs IPMN-HD (CIS) and MI-IPMC		
rMPD or rMixed type	4.92 (1.75–13.8)	0.003
Mural nodule or thick septum (+)	2.97 (1.08–8.14)	0.035
rIPMN size >40 mm	2.88 (1.04–8.02)	0.042
IPMN-HD (CIS) vs MI-IPMC		
rMPD or rMixed type	5.33 (1.54–18.5)	0.008

*Logistic regression analysis (backward stepwise method).
†CT images obtained using both single-slice helical CT and MDCT.

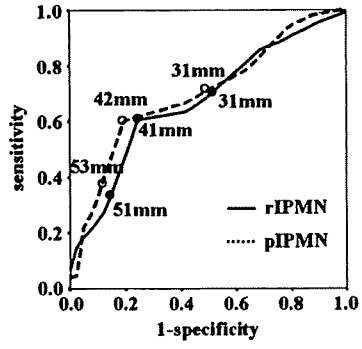

FIGURE 3. The ROC curves of rIPMN and pIPMN size. The optimal cutoff values of rIPMN and pIPMN size for detection of malignancy (carcinoma positive in a lesion) were 41 and 42 mm, respectively.

that the presence of invasive cancer detected on CT (both single-slice helical CT and MDCT) and CA-19-9 greater than 37 U/mL were significant predictive variables for IC-IPMC (Table 3).

We then analyzed how precisely CT was able to detect invasive cancers in patients with IC-IPMC. Among the 71 patients who underwent MDCT, the presence of IC-IPMC was detected with 86% sensitivity and 100% specificity, whereas single-slice helical CT (n = 52) showed 70% sensitivity and 90% specificity. Thus, the overall sensitivity and specificity of CT (n = 123) to detect invasive cancer in patients with IC-IPMC were 81% and 96%, respectively (Table 4).

Preoperative Evaluation of IPMNs Other Than IC-IPMC

We investigated the clinical and radiological findings correlated with subtypes of IPMN other than IC-IPMC (n = 92; Table 2). We excluded IC-IPMCs in which invasive cancer was not detected by CT because we aimed to clarify the characteristics of pathologically proven IPMN-HD (CIS) and MI-IPMC. Our previous study showed no significant difference in the postoperative outcome between patients with noninvasive IPMN and MI-IPMC, although 2 of 26 patients with MI-IPMC experienced recurrence.[23] Other groups also reported that 2 of 17 patients with noninvasive IPMC (IPMN-HD [CIS]) had recurrent invasive carcinoma,[13] and that 1 of 14 patients with noninvasive IPMC (IPMN-HD [CIS]) and 1 of 6 patients with MI-IPMC had recurrence after surgery.[22] Thus, preoperative detection of IPMN-HD (CIS) and MI-IPMC is a clinically important consideration, as much as the detection of IC-IPMC. The optimal cutoff values of rIPMN and pIPMN size for the detection of malignancy (IPMN-HD [CIS] and MI-IPMC) were determined to be 41 and 42 mm, respectively, on the basis of the ROC curve (Fig. 3); therefore, we adopted a cutoff value of 40 mm for rIPMN size. Univariate analysis showed that the following variables were significantly associated with malignant IPMC other than IC-IPMC: rIPMN size greater than 40 mm, rMPD diameter greater than 8 mm, rMPD or rMixed type, and the presence of a mural nodule or thick septum (Table 2). Multivariate analysis showed that rIPMN size greater than 40 mm, rMPD or rMixed type, and the presence of a mural nodule or thick septum were significant predictive factors of malignancy (Table 3).

Effectiveness of Diagnostic Score for Prediction of Noninvasive IPMC and MI-IPMC

It was unlikely that any of these preoperative variables (Table 3) alone would facilitate the accurate prediction of IPMN pathological subtypes (Table 2); therefore, we tried to predict the pathological subtypes of IPMN accurately by combining 3 variables: rIPMN size, rIPMN duct type, and the presence of a mural nodule or thick septum. A diagnostic score was devised with the aim of preoperatively identifying patients at high risk for malignancy among patients with IPMN other than IC-IPMC. The score was calculated by assigning 1 point for each of rIPMN size greater than 40 mm, rMPD or rMixed type, and mural nodule or thick septum detected on preoperative images (Table 5). The rates of malignancy (ie, IPMN-HD [CIS] and MI-IPMC) were 14%, 44%, 75%, and 86% in the patient groups with diagnostic scores of 0, 1, 2, and 3, respectively. The risk ratio of carcinoma among patients with a score 2 or 3 was 3.3 (95% confidence interval [CI], 1.8–6.0).

Comparison between IPMN-HD (CIS) and MI-IPMC showed that tumor distribution in 2 or 3 segments, MPD diameter greater than 8 mm, and rMPD or rMixed type were significantly associated with MI-IPMC by univariate analysis (Table 2), and rMPD or rMixed type remained significant by multivariate analysis (Table 3). The rates of minimal invasion were 5%, 24%, 38%, and 64% in the patient groups with diagnostic scores of 0, 1, 2, and 3, respectively (Table 5). The risk ratio of minimal invasion among patients with a score of 3 was 3.6 (95% CI, 1.7–7.7).

TABLE 5. Diagnostic Score and Results in Patients With IPMN Other Than IC-IPMC (n = 92)

A. Diagnostic score (the sum of acquired points)

Predictive variables	Acquired point
rMPD or rMixed type	Yes, 1; No, 0
Presence of mural nodule or thick septum	Yes, 1; No, 0
rIPMN size >40 mm	Yes, 1; No, 0

B. Comparison of diagnostic score between patients with benign IPMN (IPMN-LD and IPMN-MD) and patients with malignant IPMN (IPMN-HD [CIS] and MI-IPMC)

Score	Benign	Malignant	Total	Risk ratio of presence of carcinoma	95% CI
0	18 (86%)	3 (14%)	21	0.13	0.042–0.42
1	14 (56%)	11 (44%)	25	0.63	0.32–1.2
2	6 (25%)	18 (75%)	24	2.4	1.1–1.5
3	3 (14%)	19 (86%)	22	5.1	1.6–16.0

C. Comparison of diagnostic score between patients with noninvasive IPMN (IPMN-LD, IPMN-MD, and IPMN-HD [CIS]) and patients with MI-IPMC

Score	Noninvasive IPMN	MI-IPMC	Total	Risk ratio of presence of carcinoma	95% CI
0	20 (95%)	1 (5%)	21	0.10	0.015–0.73
1	19 (76%)	6 (24%)	25	0.65	0.29–1.5
2	15 (63%)	9 (38%)	24	1.2	0.61–2.5
3	8 (36%)	14 (64%)	22	3.6	1.7–7.7

Numbers in parentheses denote the percentage of the number in the *Total* column.

DISCUSSION

Recent studies on the natural history of IPMNs have revealed that the prevalence of malignancy is substantially low in small (<3 cm) BD-type IPMNs without mural nodules[27] and that it takes a relatively long period until noninvasive IPMNs progress to invasive IPMCs.[28] In addition, the current consensus regarding the malignant potential of IPMN is that its aggressiveness is dependent on the presence of invasive cancer, the extent of cancer invasion, and the biological characteristics of cancer cells.[13–19] Furthermore, MI-IPMC shows nonaggressive characteristics similar to noninvasive IPMN, whereas IC-IPMC has aggressive characteristics comparable to conventional ductal carcinoma of the pancreas.[23] These findings suggest that the therapeutic strategy for IPMN ought to differ according to the grade. Conservative treatment may be possible in selected cases of early-stage noninvasive IPMN.[29] Function-preserving pancreatectomy may be a treatment option in some noninvasive IPMNs.[30] On the other hand, as IC-IPMCs are often associated with LN metastasis[22,23] (an incidence of 61% at our institution), radical pancreatectomy with LN dissection is necessary for curative resection. Therefore, it is becoming more important to

categorize IPMN preoperatively into its corresponding pathological subtypes accurately.

Here, we retrospectively studied 123 patients who underwent surgical resection of IPMN and analyzed which preoperative findings could precisely predict the pathological subtypes. We found that MDCT was able to detect the presence of invasive cancer in IC-IPMC with 86% sensitivity and 100% specificity. We also found that rIPMN size greater than 40 mm, rMPD or rMixed type, and the presence of a mural nodule or thick septum were significant predictive factors of malignancy by multivariate analysis in patients with IPMNs other than IC-IPMC. Furthermore, the diagnostic score obtained using these 3 predictive factors showed a good correlation with the presence of carcinoma.

The clinical and radiological features of IC-IPMC are substantially different from other IPMNs. The IC-IPMCs are frequently associated with high levels of serum CA-19-9, and the invasive component of IC-IPMCs is frequently visible on CT (Table 3). These features of IC-IPMC, combined with the poor postoperative prognosis and high rate of LN metastasis, indicate that we should separate IC-IPMC from other IPMNs and treat them similarly to conventional invasive ductal carcinoma of the pancreas. When IC-IPMC is present, aggressive treatment ordinarily applied to the conventional pancreatic cancer may be indicated. This is in marked contrast with the fact that LN metastasis is almost zero in noninvasive IPMC or MI-IPMCs, and function-preserving surgery could be indicated for this patient group. Thus, we think clinicians should pay more attention to detect an associated invasive carcinoma (IC-IPMC) at initial diagnosis of IPMN.

On the basis of these findings, we propose a 2-step algorithm for determining the therapeutic strategy for patients with IPMN (Fig. 4). For the first step, patients with IPMN are categorized according to whether MDCT reveals an invasive cancer (IC-IPMC) in the lesion. For the second step, patients with IPMN other than IC-IPMC are categorized according to whether the diagnostic score suggests the presence of malignancy (Table 5). The malignancy rate was significantly high (risk ratio, 3.3; $P < 0.001$) in patients with a diagnostic score of 2 or 3. Malignancy in IPMN was detected in patients with a diagnostic score of 2 or 3, with 73% sensitivity and 78% specificity; thus, these patients should be taken to an immediate surgical operation to resect the IPMN. For patients with a diagnostic score of 1, resection is advocated for low-risk patients with a reasonable life expectancy, considering that about half (44%) of this patient group had carcinoma, although the relative risk of malignancy is lower than in patients with a diagnostic score of 2 or 3. Patients with a diagnostic score of 0 had the lowest risk of malignancy (0.13 [95% CI, 0.042–0.42]). In our series, the diagnostic score of 0 indicated IPMN as a benign lesion with 44% sensitivity and 94% specificity. Combined with previous reports showing a low occurrence rate of invasive cancer in this patient group,[28,29] these findings suggest that careful nonoperative management may be applicable for selected patients, especially those who are older or have severe complications; however, it should not be ignored that 3 (14%) of 21 patients in this group harbored carcinoma (Table 5B). Thus, "wait-and-watch" management is not always recommended for patients with a diagnostic sore of 0, and conservative treatment may be applicable in selected cases with well-informed consent about the risk of malignancy. Further accumulation of patients' follow-up data on the natural history of IPMN or the emergence of new accurate molecular markers is necessary to establish more relevant criteria for the observation strategy. Currently, balancing the malignant potential of IPMN with the risk of surgery and life expectancy may be the most practical approach for determining the indication and extent of surgery.

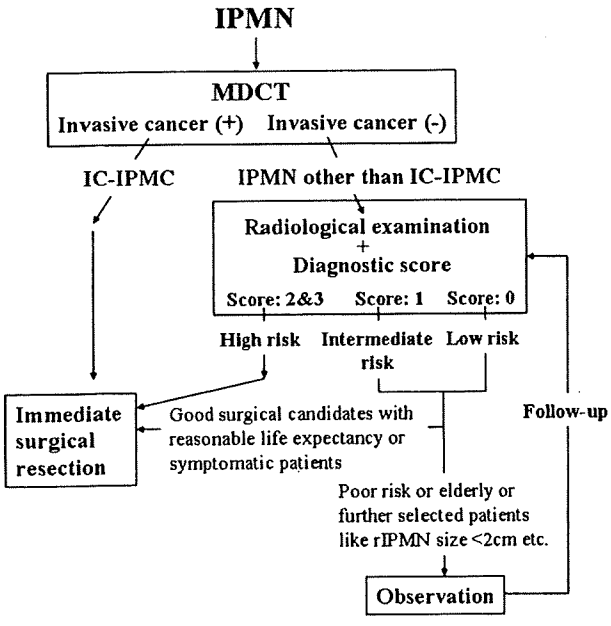

FIGURE 4. Proposed treatment algorithm for preoperative evaluation of patients with IPMN.

In this study, we were able to detect a component of invasive carcinoma in IC-IPMC using MDCT, with 86% sensitivity and 100% specificity, regardless of the size of invasive cancer. This is compatible with a recent report from another group, in which MDCT detected invasive IPMN with high sensitivity and specificity.[25] Although some authors have emphasized the diagnostic advantage of MRCP for the detection of cystic lesions,[31,32] its ability to detect solid invasive cancer associated with IPMN has not been well established. Other authors have reported that MDCT has marked ability to detect small conventional invasive cancers of the pancreas.[33,34] Although we have not yet compared the abilities of MDCT with those of MRCP for the detection of IC-IPMC, the present study has provided evidence that MDCT is very useful for the accurate detection of IC-IPMC. In our series, MDCT produced no false-positive images of patients with IC-IPMC, although it is possible that inflammatory change in the adjacent pancreatic parenchyma may be misdiagnosed as invasive cancer, as has been reported in cases of conventional invasive cancer of the pancreas.[35] Furthermore, the invasion of mucinous carcinoma may be misinterpreted as an ordinary cystic lesion without invasion.

Pathological examination revealed that IPMNs formed cystic or macroscopically papillary lesions and often spread to the surrounding pancreatic ducts. Low papillary features or spreading to minimally dilated ducts was also evident. To assess the size of IPMN on CT images, we carefully inspected the subtle signs corresponding to their features, especially papillary projection into the pancreatic duct, which has been reported to reflect the lateral spreading of low papillary lesions.[24] We examined the accuracy of radiological evaluation such as the size of rIPMN and the rIPMN duct type by comparison with pIPMN size and pIPMN duct type, respectively, using 92 IPMNs other than IC-IPMC. The size of rIPMN was measured fairly accurately and corresponded to the size of pIPMN ± 20% in 92.4% of cases and to the size of pIPMN ± 10% in 67.4% of cases. The rIPMN duct type was correctly evaluated in all but 7% of

IPMN cases. To improve the accuracy of such preoperative evaluation, additional examinations such as endoscopic retrograde cholangiopancreatography, endoscopic US, and magnetic resonance imaging may be helpful to reveal the more detailed characteristics of the lesion, if precise assessment of a laterally spreading lesion is difficult using MDCT. The discrepancy between imaging data and pathological findings may be 1 reason why intraoperative frozen-section analysis is necessary to secure a tumor-free margin.[36]

Historically, there were few reports mentioning about the radiological size of rMPD-type IPMN, and only MPD diameter has been measured.[10,17] The reason may be because the size of rMPD-type IPMN was difficult to be measured radiologically, especially those that are not macroscopically cystic and only accompanied with a diffusely dilated MPD. However, the recent advancement of radiological examinations, especially high-spatial resolution MDCT, makes it possible to evaluate the horizontal extension of intraductal epithelial lesion in the hepatobiliary-pancreatic region. For example, a high diagnostic accuracy of horizontal spreading of hilar cholangiocarcinoma by MDCT is reported.[37] In this study, we deliberately assessed the size of rMPD-type IPMNs, taking into account lateral spreading of papillary lesions, which is reflected on subtle brushlike appearance along the wall of pancreatic ducts (Figs. 2A, B). Measuring the radiological size of all IPMNs on CT images, we could conduct the analysis without separating rBD-type from rMPD/mixed-type IPMN. In addition, our diagnostic score (Table 5A) calculates an extensive MPD-type IPMN (>4 cm in size) as a score of 2 or more and indicates an immediate resection in a surgically fit patient, according to our treatment algorithm (Fig. 4). This is in line with the international consensus guideline,[6] in which all the MPD-type IPMNs are recommended to resection. Thus, actually, the discrimination between BD type and MPD/mixed type is integrated in our scoring system, together with the other 2 predictors (IPMN size and the presence of mural nodule or thick septum).

The number of patients with multifocal IPMNs is relatively small (5 patients) perhaps because the lesion was diagnosed as multiple only when multiple IPMNs were demonstrated pathologically in the resected specimen. For example, when a patient who had 2 suspected IPMN lesions in the pancreatic head and tail underwent pancreaticoduodenectomy and the resected specimen revealed a single IPMN in the pancreatic head, the patient was recognized as having a single IPMN lesion in our analysis because the diagnosis of the tail lesion has not been acquired pathologically.

This study was limited in that it was retrospective and evaluated the predictive ability of CT images for lesions known to be IPMNs. In addition, the study population is composed only of patients who underwent surgical resection. We intend to test our preoperative diagnostic algorithm using another large series of samples or in a prospective study.

ACKNOWLEDGMENT

The authors thank Dr Hidenori Ojima for useful discussions.

REFERENCES

1. Hruban RH, Pitman MB, Klimstra DS. *AFIP Atlas of Tumor Pathology Fourth Series Fascicle 6: Tumor of the Pancreas*. Washington, DC: American Registry of Pathology; 2007:75–110.
2. Longnecker DS, Adler G, Hruban RH, et al. Intraductal papillary-mucinous neoplasms of the pancreas. In: Hamilton SR, Aaltonen LA, eds. *Pathology and Genetics. Tumours of the Digestive System. World Health Organization Classification of Tumours*. Lyon, France: IARC Press; 2000:237–240.
3. Biankin AV, Kench JG, Dijkman FP, et al. Molecular pathogenesis of precursor lesions of pancreatic ductal adenocarcinoma. *Pathology*. 2003;35:14–24.
4. Hruban RH, Takaori K, Klimstra DS, et al. An illustrated consensus on the classification of pancreatic intraepithelial neoplasia and intraductal papillary mucinous neoplasms. *Am J Surg Pathol*. 2004;28:977–987.
5. Hiraoka N, Onozato K, Kosuge T, et al. Prevalence of FOXP3$^+$ regulatory T cells increases during the progression of pancreatic ductal adenocarcinoma and its precursor lesions. *Clin Cancer Res*. 2006;12:5423–5434.
6. Tanaka M, Chari S, Adsay V, et al. International consensus guidelines for management of intraductal papillary mucinous neoplasms and mucinous cystic neoplasms of the pancreas. *Pancreatology*. 2005;6:17–32.
7. Sakorafas GH, Sarr MG, van de Velde CJ, et al. Intraductal papillary mucinous neoplasms of the pancreas: a surgical perspective. *Surg Oncol*. 2005;14:155–178.
8. Murakami Y, Uemura K, Hayashidani Y, et al. Predictive factors of malignant or invasive intraductal papillary-mucinous neoplasms of the pancreas. *J Gastrointest Surg*. 2007;11:338–344.
9. Hara T, Yamaguchi T, Ishihara T, et al. Diagnosis and patient management of intraductal papillary-mucinous tumor of the pancreas by using peroral pancreatoscopy and intraductal ultrasonography. *Gastroenterology*. 2002;122:33–43.
10. Sugiyama M, Izumisato Y, Abe N, et al. Predictive factors for malignancy in intraductal papillary-mucinous tumours of the pancreas. *Br J Surg*. 2003;90:1244–1249.
11. Jang JY, Kim SW, Ahn YJ, et al. Multicenter analysis of clinicopathologic features of intraductal papillary mucinous tumor of the pancreas: is it possible to predict the malignancy before surgery? *Ann Surg Oncol*. 2005;12:124–132.
12. Sahani DV, Kadavigere R, Blake M, et al. Intraductal papillary mucinous neoplasm of pancreas: multi-detector row CT with 2D curved reformations—correlation with MRCP. *Radiology*. 2006;238:560–569.
13. Chari ST, Yadav D, Smyrk TC, et al. Study of recurrence after surgical resection of intraductal papillary mucinous neoplasm of the pancreas. *Gastroenterology*. 2002;123:1500–1507.
14. D'Angelica M, Brennan MF, Suriawinata AA, et al. Intraductal papillary mucinous neoplasms of the pancreas: an analysis of clinicopathologic features and outcome. *Ann Surg*. 2004;239:400–408.
15. Maire F, Hammel P, Terris B, et al. Prognosis of malignant intraductal papillary mucinous tumours of the pancreas after surgical resection. Comparison with pancreatic ductal adenocarcinoma. *Gut*. 2002;51:717–722.
16. Raimondo M, Tachibana I, Urrutia R, et al. Invasive cancer and survival of intraductal papillary mucinous tumors of the pancreas. *Am J Gastroenterol*. 2002;97:2553–2558.
17. Salvia R, Fernandez-del Castillo C, Bassi C, et al. Main-duct intraductal papillary mucinous neoplasms of the pancreas: clinical predictors of malignancy and long-term survival following resection. *Ann Surg*. 2004;239:678–687.
18. Shimada K, Sakamoto Y, Sano T, et al. Invasive carcinoma originating in an intraductal papillary mucinous neoplasm of the pancreas: a clinicopathologic comparison with a common type of invasive ductal carcinoma. *Pancreas*. 2006;32:281–287.
19. Sohn TA, Yeo CJ, Cameron JL, et al. Intraductal papillary mucinous neoplasms of the pancreas: an updated experience. *Ann Surg*. 2004;239:788–789.
20. Japan Pancreas Society. *Classification of Pancreatic Cancer*. 2nd ed. Tokyo: Kanehara; 2003.

21. Suzuki Y, Atomi Y, Sugiyama M, et al. Cystic neoplasm of the pancreas: a Japanese multiinstitutional study of intraductal papillary mucinous tumor and mucinous cystic tumor. *Pancreas*. 2004;28:241–246.
22. Nakagohri T, Kinoshita T, Konishi M, et al. Surgical outcome of intraductal papillary mucinous neoplasms of the pancreas. *Ann Surg Oncol*. 2007;14:3174–3180.
23. Nara S, Shimada K, Kosuge T, et al. Minimally invasive intraductal papillary-mucinous carcinoma of the pancreas: clinicopathological study of 104 intraductal papillary-mucinous neoplasms. *Am J Surg Pathol*. 2008;32:243–255.
24. Itai Y, Minami M. Intraductal papillary-mucinous tumor and mucinous cystic neoplasm: CT and MR findings. *Int J Gastrointest Cancer*. 2001;30:47–63.
25. Kawamoto S, Lawler LP, Horton KM, et al. MDCT of intraductal papillary mucinous neoplasm of the pancreas: evaluation of features predictive of invasive carcinoma. *Am J Roentgenol*. 2006;186:687–695.
26. Nakagohri T, Konishi M, Inoue K, et al. Invasive carcinoma derived from intraductal papillary mucinous carcinoma of the pancreas. *Hepatogastroenterology*. 2004;51:1480–1483.
27. Matsumoto T, Aramaki M, Yada K, et al. Optimal management of the branch duct type intraductal papillary mucinous neoplasms of the pancreas. *J Clin Gastroenterol*. 2003;36:261–265.
28. Kobayashi G, Fujita N, Noda Y, et al. Mode of progression of intraductal papillary-mucinous tumor of the pancreas: analysis of patients with follow-up by EUS. *J Gastroenterol*. 2005;40:744–751.
29. Salvia R, Crippa S, Falconi M, et al. Branch-duct intraductal papillary mucinous neoplasms of the pancreas: to operate or not to operate? *Gut*. 2006;56:1086–1090.
30. Kimura W. IHPBA in Tokyo, 2002: surgical treatment of IPMT vs MCT: a Japanese experience. *J Hepatobiliary Pancreat Surg*. 2003;10:156–162.
31. Sugiyama M, Atomi Y, Hachiya J. Intraductal papillary tumors of the pancreas: evaluation with magnetic resonance cholangiopancreatography. *Am J Gastroenterol*. 1998;93:156–159.
32. Irie H, Honda H, Aibe H, et al. MR cholangiopancreatographic differentiation of benign and malignant intraductal mucin-producing tumors of the pancreas. *Am J Roentgenol*. 2000;174:1403–1408.
33. Scaglione M, Pinto A, Romano S, et al. Using multidetector row computed tomography to diagnose and stage pancreatic carcinoma: the problems and the possibilities. *J Pancreas*. 2005;6:1–5.
34. Prokesch RW, Schima W, Chow LC, et al. Multidetector CT of pancreatic adenocarcinoma: diagnostic advances and therapeutic relevance. *Eur Radiol*. 2003;13:2147–2154.
35. Balthazar EJ. Pancreatitis associated with pancreatic carcinoma. *Pancreatology*. 2005;5:330–344.
36. Couvelard A, Sauvanet A, Kianmanesh R, et al. Frozen sectioning of the pancreatic cut surface during resection of intraductal papillary mucinous neoplasms of the pancreas is useful and reliable. *Ann Surg*. 2005;242:774–778.
37. Unno M, Okumoto T, Katayose Y, et al. Preoperative assessment of hilar cholangiocarcinoma by multidetector row computed tomography. *J Hepatobiliary Pancreat Surg*. 2007;14:434–440.

Langenbecks Arch Surg (2009) 394:1115–1121
DOI 10.1007/s00423-009-0500-1

HOW TO DO IT

Reconstruction of the portal and hepatic veins using venous grafts customized from the bilateral gonadal veins

Yusuke Yamamoto · Yoshihiro Sakamoto · Satoshi Nara · Daisuke Ban · Minoru Esaki · Kazuaki Shimada · Tomoo Kosuge

Received: 9 March 2009 / Accepted: 20 April 2009 / Published online: 7 May 2009

Abstract
Background Surgical resection for pancreatic and hepatic cancer sometimes involves combined resection and reconstruction of the major veins using venous grafts. Autologous venous grafts made from the bilateral gonadal veins (BGVs) have never been utilized or discussed.
Materials and methods We reconstructed the portal vein (PV), superior mesenteric vein (SMV), and middle hepatic vein (MHV) using cylindrical or patch grafts customized from the BGVs in two female patients and in one male patient. In order to assess the sexual difference in the availability of the cylindrical graft to replace these major veins, we measured the diameters of the BGVs, PV, SMV, and MHV on computed tomography in 50 male and 50 female patients, and estimated the diameter-ratios (DRs) of the cylindrical graft made from BGVs/PV, SMV, and MHV. We assumed that the cutoff value of the DR would be 0.8, for replacing of major veins using cylindrical grafts.
Results The reconstructed PV, SMV, and MHV presented sufficient patency, and the postoperative courses were uneventful. The DRs of BGVs graft/PV, graft/SMV, and graft/MHV were significantly larger in female patients than those in male patients (0.82 vs. 0.54, $p<0.01$, 0.96 vs. 0.61, $p<0.01$, 1.39 vs. 0.95; $p<0.01$) and were larger than 0.8 in 50%, 70%, and 92% in female patients, respectively, and 0%, 8%, and 68% in male patients, respectively.
Conclusions The present newly customized cylindrical and patch grafts made from the BGVs showed sufficient feasibility. A cylindrical graft made from the BGVs would be better utilized in female patients than in male patients.

Keywords Gonadal vein · Venous graft · Reconstruction · Pancreaticoduodenectomy · Hepatectomy

Y. Yamamoto · Y. Sakamoto (✉) · S. Nara · D. Ban · M. Esaki · K. Shimada · T. Kosuge
Hepatobiliary and Pancreatic Surgery Division,
National Cancer Center Hospital,
5-1-1Tsukiji, Chuo-ku,
Tokyo 104-0045, Japan
e-mail: yosakamo@ncc.go.jp

Introduction

Pancreatic and hepatic cancers often infiltrate the portal vein (PV), superior mesenteric vein (SMV), and hepatic veins (HVs), and curative resection of these tumors sometimes involves combined resection of the PV, SMV, and HVs with pancreatectomy and hepatectomy. When the venous defect on the PV or HVs is small, direct suturing would be the most simple and time-preserving method. PV reconstruction during pancreaticoduodenectomy can be performed by direct suturing or direct anastomosis between the PV and SMV without any interposition graft. However, when a direct suturing or direct anastomosis has some risks of kinking, stenosis, or overtension, a venous graft will be necessary. Some authors have reported the usefulness of autologous venous grafts created from the internal jugular vein [1, 2], left renal vein (LRV) [3–9], external iliac vein [10–14], and superficial femoral vein [11]. Others have utilized customized venous grafts made from lesser veins, such as the great saphenous vein [10, 11, 15–17] or right ovarian vein [18], to avoid deficiency or complications associated with sacrificing intrinsic thicker veins. However, the creation of venous grafts using the bilateral gonadal veins (BGVs) has never been reported previously.

In the present paper, we describe three cases of reconstruction of the PV, SMV, and HV, using venous grafts customized from the BGVs. Furthermore, we assessed the sexual difference in the availability of the cylindrical grafts custom-

ized from the BGVs to replace the PV, SMV, and HVs, in terms of the diameter of the graft relative to each vein, based on analysis of 100 computed tomographic (CT) images.

Materials and methods

We performed resection and reconstruction of the PV and SMV using a patch graft in one female patient and a cylindrical graft in another female patient customized from the BGVs during pancreaticoduodenectomy for pancreatic cancer and reconstruction of the middle hepatic vein (MHV) using a cylindrical graft customized from the BGVs during multiple partial hepatectomies for removal of metastatic rectal cancers in one male patient. Table 1 shows the patient characteristics and the venous diameters on CT scan.

Techniques of reconstruction of the PV, SMV, and MHV using venous grafts customized from the BGVs

In cases 1 and 2, we performed pancreaticoduodenectomy combined with resection of the PV or SMV for the treatment of pancreatic head cancer. Before resection of the PV or SMV with the specimen, we harvested the BGVs and cut them longitudinally (Fig. 1a). The two pieces from the BGVs were sutured side-by-side intermittently using 6-0 prolene, to obtain a larger sheet (Fig. 1b). In case 1, we sutured the two edges of the defect transversely before patch reconstruction because the defect of the PV was larger than we expected. The sheet graft was patched on the defect with a running suture using 5-0 prolene (Fig. 1c). In case 2, we wrapped the sheet around a 24Fr drain tube longitudinally and sutured it side-by-side intermittently using 6-0 prolene, to make a cylindrical graft. The finished graft was interposed in the venous defect for reconstruction of the SMV with running sutures using 6-0 prolene (Fig. 1d).

In case 3, a male patient had six metastatic hepatic tumors from rectal cancer, and one of these tumors involved the MHV. He underwent preoperative systemic chemotherapy using irinotecan and oxaliplatin, intravenous fluorouracil, and leucovorin for 1 year and additional hepatic arterial infusion therapy with fluorouracil. We performed six partial hepatectomies and combined with resection of the MHV. On CT scan, the diameter ratio (DR) of the sum of the diameters of the BGVs to the diameter of the MHV (BGVs graft/MHV) was 0.72 (Table 1), the cylindrical graft made from the two pieces of the BGVs was supposed to be insufficient to replace the MHV. After dividing the liver parenchyma around the MHV, we harvested the right GV, 7.0 cm in length, and the left GV, 5.0 cm in length, and cut them longitudinally (Fig. 1e). We divided the right GV into two half-length pieces, 3.5 cm in length, and divided left GV into two pieces, 3.5 cm×1.0 cm in size. We wrapped the three pieces of the BGVs, 3.5 cm in length, around a 24Fr drain tube longitudinally and sutured them side-by-side intermittently using 7-0 prolene to make a cylindrical graft, with a diameter of 1.0 cm and a length of 3.5 cm. We segmentally removed the MHV for 3 cm in length and interposed the cylindrical graft with running suture using 6-0 prolene (Fig. 1f). We did not perform anticoagulant therapy in these three patients.

Analysis of the diameters of the BGVs, PV, SMV, and HVs on CT images

The clinical records and CT images of the patients who visited our outpatient clinic from August 2007 to July 2008 were reviewed retrospectively. Patients who had history of abdominal surgery, gynecologic surgery, or portal hypertension with blood platelet counts less than 100,000 per microliter were excluded from this study. The underlying disease in the 100 patients included pancreatic head cancer (n=42), pancreatic body or tail cancer (n=13), distal bile duct cancer (n=3), hilar bile duct cancer (n=6), gallbladder cancer (n=1), duodenal cancer (n=1), hepatocellular carcinoma (n=14), intrahepatic cholangiocarcinoma (n=8), intraductal papillary mucinous tumor of pancreas (n=2), pancreatic endocrine tumor (n=4), retroperitoneal tumor (n=3), other hepatic tumor (n=2), and pancreatitis (n=1). There were 50 men and 50 women, with a mean age of 63 years (range, 33–81 years). A 16-row multidetector scanner (Aquilion V-detector, Toshiba Medical Systems, Tokyo, Japan) was used in all the patients with intravenous contrast injection. CT scans were obtained during the arterial phase (40-s delay), portal venous phase (70-s delay), and equilibrium phase (3-min delay) after intravenous administration, at section thicknesses of 1 and 5 mm and intervals of 1 and 5 mm through the abdomen and pelvis.

We measured the maximum diameters of the BGVs, PV, SMV, right hepatic vein (RHV), MHV, and left hepatic vein (LHV) in the transverse images in each patient. The diameters of the PV and SMV were measured at the level of the superior and inferior borders of the pancreas, respectively. The diameters of the three HVs were measured at the confluence with the inferior vena cava.

We studied the sexual differences in the diameters of the BGVs, PV, SMV, and HVs, and also examined the sexual differences in the DRs of the sum of the diameters of the BGVs to the diameter of the PV, SMV, and HVs (BGVs graft/PV, graft/SMV, and graft/HVs), in order to investigate whether cylindrical venous grafts prepared from the BGVs were suitable for bridging of the venous defect in the PV, SMV, and HVs. We assumed that the acceptable cutoff value of the DR of the graft/PV, graft/SMV, or graft/HVs would be 0.8, for safe replacing of the PV, SMV, or HVs using the cylindrical graft made from the BGVs.

Data were entered into a computer database and statistically analyzed using SPSS for Windows (version

Table 1 Patient characteristics and the venous diameters on computed tomography scan in three patients undergoing venous reconstruction using the bilateral gonadal veins

Case	Age/ sex	Disease	Tumor size (mm)	Involved vein	Involved length (mm)	Diameters on CT scan (mm)						Diameter-ratio		
						PV	SMV	MHV	RGV	LGV	Sum of BGVs	BGVs/ MHV	BGVs/ PV	BGVs/ SMV
1	66/F	PC	33	PV	30	11.7	7.3	–	2.9	4.5	7.4	0.63	1.01	–
2	50/F	PC	40	SMV	35	12.2	7.5	–	3.4	3.4	6.8	0.55	0.89	–
3	59/M	LM	40	MHV	30	–	–	9.4	3.5	3.3	6.8	–	–	0.72

PC pancreatic invasive cancer, *LM*, liver metastasis, *PV* portal vein, *SMV* superior mesenteric vein, *MHV* middle hepatic vein, *CT* scan computed tomography scan, *RGV* right gonadal vein, *LGV* left gonadal vein, *BGVs* bilateral gonadal veins, *BGVs/PV* the diameter-ratio of the sum of the BGVs to the PV, *BGVs/SMV* the diameter-ratio of the sum of the BGVs to the SMV, *BGVs/MHV* the diameter-ratio of the sum of the BGVs to the MHV

11.5; SPSS, Chicago, IL, USA). The summarized data were formatted as mean±standard deviation (SD). Statistical analysis was evaluated using the paired Student's *t* test for parametrically distributed data and the Wilcoxon matched-pair signed-rank test for nonparametrically distributed data. $P<0.05$ was considered to be statistically significant.

Results

All of the three patients undergoing reconstruction of the PV, SMV, and MHV using venous grafts customized from the BGVs had uneventful perioperative courses. Table 2 shows the surgical results of the three patients. Good patency

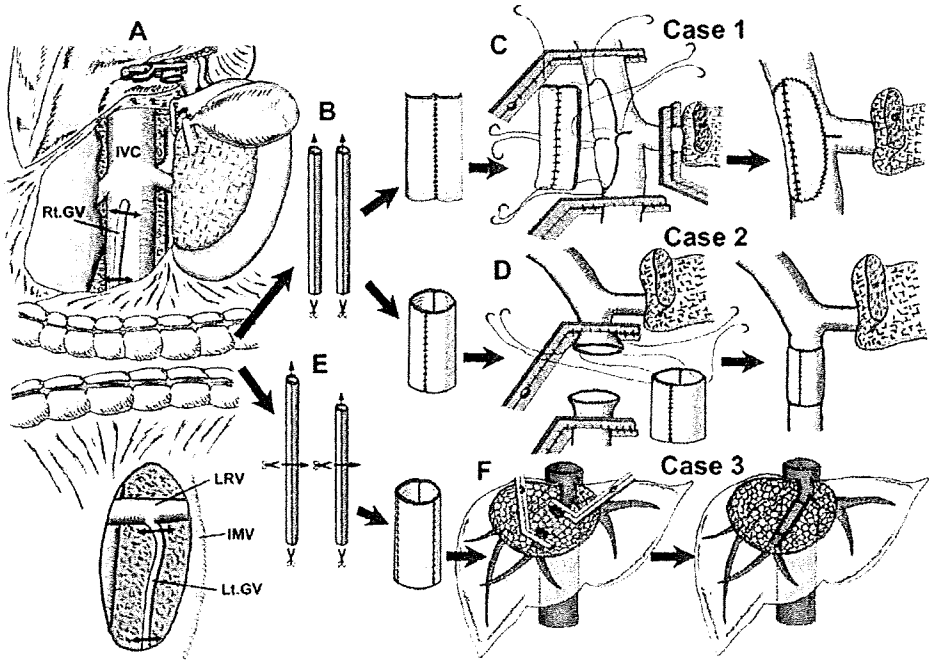

Fig. 1 Schematic illustration of reconstruction of the portal vein (PV), superior mesenteric vein (SMV), and middle hepatic vein (MHV) using grafts customized from the bilateral gonadal veins (BGVs). *A* The proximal side of the BGVs was sacrificed. *B* Sacrificed BGVs were cut longitudinally. The two pieces obtained were sutured intermittently side-by-side using 6-0 prolene, to make a sheet graft. *C* The obtained sheet graft was patched on to the defect of the PV with a running suture using 5-0 prolene. Before patching the graft, both edges of the PV defect were sutured for a length of 1 cm to reduce the size of the defect. *D* The obtained sheet was rolled around a 24Fr drain tube and sutured side-by-side intermittently using 6-0 prolene. The finished cylindrical graft was interposed to reconstruct the SMV with a running suture using 6-0 prolene. *E* We harvested the right GV, 7.0 cm in length, and the left GV, 5 cm in length, and cut them longitudinally. We divided right GV into two equal parts, 3.5 cm in length, and divided left GV into two parts, 3.5 cm × 1.0 cm in size, respectively. *F* We wrapped these three pieces with length of 3.5 cm around a 24Fr drain tube longitudinally and sutured them side-by-side intermittently using 7-0 prolene to make a cylindrical graft. We interposed the cylindrical graft in the venous defect for reconstruction of the MHV with running suture using 6-0 prolene. *IVC* inferior vena cava, *Rt.GV* right gonadal vein, *LRV* left renal vein, *IMV* inferior mesenteric vein, *Lt.GV* left gonadal vein

of the reconstructed veins was confirmed in follow-up CT scans, 5, 1, and 1 months after the surgery, respectively. None of the patients developed any complication associated with sacrificing the BGVs.

The BGVs, PV, SMV, and HVs were visualized in all the 100 patients on CT images. The right GV joined to the right renal vein in six patients and to the inferior vena cava in 94 patients. The left GV was joined to the LRV in all patients. Table 3 shows the sexual differences in the diameters of the right, left, and BGVs, PV, SMV, and HVs. The diameters of right, left, and BGVs were significantly larger in female patients than in male patients (p=0.02, <0.01, <0.01). On the other hand, the diameters of the PV, SMV, and MHV were significantly smaller in female patients than in male patients (p<0.01, <0.01, <0.01). There were no significant differences between the male and female patients in the diameter of the RHV and LHV. The left GV was significantly larger than the right GV in female patients (p<0.01), while there was no significant difference in the diameter between the right and left GVs in male patients (p=0.50).

Figure 2 shows the box plots of the DRs of the sum of the diameters of the BGVs to the diameters of the PV, SMV, and MHV. The DRs of BGVs graft/ PV, graft/SMV, and graft/MHV were significantly greater in female patients than in male patients (DR of BGVs graft/PV, 0.82±0.22 vs. 0.54±0.09; DR of BGVs graft/SMV, 0.94±0.26 vs. 0.61± 0.13; DR of BGVs graft/MHV, 1.39±0.53 vs. 0.95±0.26; p<0.01, <0.01, <0.01).

The DRs of BGVs graft/PV and graft/SMV were larger than 0.8 in 50% and 70% in female patients, respectively, and 0% and 8% in male patients, respectively. The DRs of BGVs graft/MHV were larger than 0.8 in 92% in female patients and 68% in male patients.

Discussion

In this report, we present the usefulness of newly developed patch and cylindrical grafts customized from the BGVs for reconstruction of the PV, SMV, or MHV. The BGVs were easily and safely excised with length of approximately 6 cm from the same surgical field without making additional incision or adverse effect. To the best of our knowledge, there has been only one report of the use of a venous patch graft made from the right ovarian vein after PV or HV wedge resection in female patients [18]. None of the three patients developed any complication associated with sacrificing the BGVs. We believe that the side effect of sacrificing the BGVs is minimal, but there are some reports of gonadal vein thrombosis presenting with lower abdominal pain [19, 20]. This issue should be further evaluated.

Analysis of the diameters on CT images revealed that cylindrical grafts prepared from two pieces of the BGVs may be too thin in about half of female patients and almost all of male patients for replacing of the PV or SMV, if we assume that the required DR of the graft might be 0.8 for safe replacing of the intrinsic veins. Cylindrical grafts prepared from the BGVs may be sufficient in almost all of female patients and about two thirds of male patients for replacing of the HVs. In case 3, as the DR of the BGVs graft/MHV was less than 0.8, we replaced a venous graft from three pieces of the BGVs and obtained a sufficient caliber. These results suggest that cylindrical venous grafts made from the BGVs could be better utilized in female patients than in male patients. It should be important to estimate the DR of the grafts/PV, graft/SMV, or graft/HV on preoperative CT scans and to plan the method of resection and reconstruction of the major intrinsic veins. If a cylindrical graft is supposed to be too thin for replacing a major vein on preoperative CT scan, (1) patch reconstruction using a sheet graft, 2) reconstruction using a cylindrical graft made from three pieces of BGVs, or 3) reconstruction using other thicker veins, would be alternatives for safe reconstruction of major veins.

In the present study, the left GV was significantly thicker than the right GV in the female patients, but not in the male patients. Hiromura et al. [21] reported that parous women had wider ovarian veins than nulliparous woman, and reflux of contrast medium from the LRV into the left ovarian vein was found in 44% (48/110) of parous women. Rebner M et al. [22] suggested that the increased venous blood flow during pregnancy might account for the enlargement of the GVs in postpartum patients. Goken et al. [23] reported that the right

Table 2 Surgical results in three patients undergoing venous reconstruction using the bilateral gonadal veins

Case	Type of the graft	Size of the sheet (mm)	Diameter of the graft (mm)	Operation time (min)	Blood loss (ml)	Graft time (min)	Clamping time (min)	Hospital stay (days)	Outcome	Survival time (months)
1	Patch	22×40	NA	590	1,100	35	53	20	Alive	5
2	Cylinder	21×30	7	620	660	32	35	35	Died of recurrence	17
3	Cylinder	35×30	10	780	1,510	50	45	17	Alive	2

graft time time required for modifying the venous graft, *clamping time* clamping time required for reconstruction of the portal vein or hepatic vein, *NA* not available

Table 3 Comparison of the diameters of the right, left, and bilateral gonadal veins, portal vein, superior mesenteric vein, right hepatic vein, middle hepatic vein, and left hepatic vein between male and female patients

Type of the vein	Mean diameter of the vein (mm, mean±SD)		*p* Value
	Female (n=50)	Male (n=50)	
Right gonadal vein	3.9±0.9	3.6±0.6	0.02
Left gonadal vein	5.3±2.0	3.6±0.8	<0.01
Sum of bilateral gonadal veins	9.3±2.5	7.2±1.2	<0.01
Portal vein	11.4±1.1	13.7±1.6	<0.01
Superior mesenteric vein	9.5±1.4	12.0±1.5	<0.01
Right hepatic vein	8.2±2.2	8.3±2.0	0.96
Middle hepatic vein	7.1±1.5	7.9±1.7	<0.01
Left hepatic vein	7.8±1.8	8.2±2.1	0.31

GV was enlarged on the CT in patients with mesenteric varices or portal hypertension. Although enlargements of the GVs may be associated with many conditions including postpartum period, pregnancy, and portal hypertension, our results clearly indicate the tendency toward enlargement of the GVs in female subjects.

The superficial femoral vein, internal jugular vein, and external iliac vein are useful alternative sources for cylindrical grafts needing no modification, but sacrificing these veins may be associated with postoperative venous congestion, although it is usually compensated. The LRV provides a graft with good caliber and is easily accessible without additional incision; however, transient renal dysfunction has been reported after ligation or transection of the LRV [6, 8, 24], LRV grafts may not be feasible in patients with poor renal or general condition. Although utility of synthetic grafts has been reported, this method might be associated with graft infection and subsequent loss [25]. The advantages of venous reconstruction using BGVs would be (1) the graft is autologous, (2) easy accessibility without additional incision, and (3) safety without any complication associated with sacrificing BGVs. The disadvantage would be that this method is time-consuming, requiring 30 min for making a cylindrical graft. Our method could be utilized even in poor risk patients.

What would be the acceptable DRs of the graft/PV, graft/SMV, or graft/HVs for bridging of the venous defect in the PV, SMV, or HVs? This is a crucial question. In case 2, the DR of the BGVs graft/SMV was 0.89, and the patency of the reconstructed SMV was confirmed at 1 month after the surgery. Therefore, we assumed that the acceptable DR of the graft/PV, graft/SMV, or graft/HV on preoperative CT would be no less than 0.8. We believe that DR of 0.8 would be a safe and acceptable threshold for replacing PV or HV without stenosis or obstruction using a cylindrical graft made from BGVs, but we must further accumulate the data and look for a better cutoff value. In case 3, the DR of the BGVs graft/MHV was 0.72; therefore, we made a thicker cylindrical graft using three pieces of BGVs, and the DR of the graft/MHV increased to 1.10. If we have rolled the three

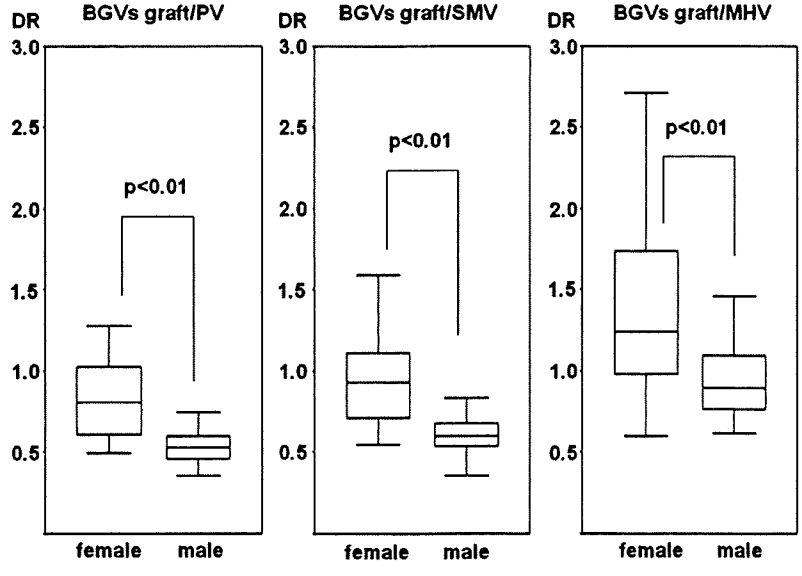

Fig. 2 Box plots of the diameter-ratios (DRs) of the sum of the bilateral gonadal veins divided by the portal vein, superior mesenteric vein, and middle hepatic vein. Diameter-ratio (DR)=The sum of the BGVs/PV, SMV, and MHV. *DR* diameter-ratio, *PV* portal vein, *BGVs* bilateral gonadal veins, *SMV* superior mesenteric vein, *MHV* middle hepatic vein

pieces of the BGVs turning sideways as previously we reported [15], we could have made a graft of a diameter of 1.1 cm and a length of 3.2 cm. This could be another option for making a longer or thicker graft.

The indication for reconstruction of the MHV might be controversial. We reconstructed the MHV in case 3 because (1) the patient had undergone preoperative chemotherapy and hepatic arterial infusion and might have potentially impaired hepatic function, and (2) we already had performed multiple partial resections of the liver and had to preserve the remnant hepatic function as far as possible. Recently, the necessity of reconstruction of the MHV has been advocated during living donor liver transplantation (LDLT) using right liver grafts [26–28]. Sano et al. [29] has demonstrated the indication for MHV reconstruction using the temporary artery occlusion test and Doppler ultrasonography. In review of the CT images, we can estimate that a cylindrical graft, 6 cm in length, could be prepared from the BGVs in almost all of the female patients and about two thirds of the male patients. Many types of venous graft have been used for the reconstruction of the MHV; the BGVs graft may be an option for reconstruction of the MHV during LDLT.

Conclusion

We presented successful three cases of major venous reconstruction using a cylindrical or patch graft customized from the BGVs. It is important to estimate the DR of the graft/the major replacing vein on preoperative CT scan and to plan the method of venous resection and reconstruction. A cylindrical graft made from the BGVs would be better utilized in female patients than in male patients.

Acknowledgments Supported in part by Grant-in-Aid for scientific research from the Ministry of Education, Science and Culture, and the Ministry of Health and Welfare of Japan

References

1. Fuhrman GM, Leach SD, Staley CA, Cusack JC, Charnsangavej C, Cleary KR, El-Naggar AK, Fenoglio CJ, Lee JE, Evans DB (1996) Rationale for en bloc vein resection in the treatment of pancreatic adenocarcinoma adherent to the superior mesenteric–portal vein confluence. Pancreatic Tumor Study Group. Ann Surg 223:154–162. doi:10.1097/00000658-199602000-00007
2. Evans DB, Lee JE, Leach SD, Fuhrman GM, Cusack JC Jr, Rich TA (1996) Vascular resection and intraoperative radiation therapy during pancreaticoduodenectomy: rationale and technique. Adv Surg 29:235–262
3. Harrison LE, Brennan MF (1997) Portal vein involvement in pancreatic cancer: a sign of unresectability? Adv Surg 31:375–394
4. Miyazaki M, Itoh H, Kaiho T, Ambiru S, Togawa A, Sasada K, Shiobara M, Shimizu Y, Yoshioka S, Yoshitome H, Nakajima N (1995) Portal vein reconstruction at the hepatic hilus using a left renal vein graft. J Am Coll Surg 180:497–498
5. Ohwada S, Hamada K, Kawate S, Sunose Y, Tomizawa N, Yamada T, Okabe T, Ogawa T, Sato Y (2007) Left renal vein graft for vascular reconstruction in abdominal malignancy. World J Surg 31:1215–1220. doi:10.1007/s00268-007-9015-5
6. Smoot RL, Christein JD, Farnell MB (2007) An innovative option for venous reconstruction after pancreaticoduodenectomy: the left renal vein. J Gastrointest Surg 11:425–431. doi:10.1007/s11605-007-0131-1
7. Choudry H, Avella D, Garcia L, Han D, Staveley-O'Carroll K, Kimchi E (2008) Use of the left renal vein as a practical conduit in superior mesenteric vein reconstruction. J Surg Res 146:117–120. doi:10.1016/j.jss.2007.07.022
8. Suzuki T, Yoshidome H, Kimura F, Shimizu H, Ohtsuka M, Kato A, Yoshitomi H, Nozawa S, Sawada S, Miyazaki M (2006) Renal function is well maintained after use of left renal vein graft for vascular reconstruction in hepatobiliary–pancreatic surgery. J Am Coll Surg 202:87–92. doi:10.1016/j.jamcollsurg.2005.08.001
9. Ohwada S, Takeyoshi I, Ogawa T, Ohya T, Saitoh A, Kawashima K, Iino Y, Morishita Y (1998) Hepatic vein reconstruction at inferior vena cava confluence using left renal vein graft. Hepatogastroenterology 45:1833–1836
10. Nakamura S, Sakaguchi S, Kitazawa T, Suzuki S, Koyano K, Muro H (1990) Hepatic vein reconstruction for preserving remnant liver function. Arch Surg 125:1455–1459
11. Nakamura S, Sakaguchi S, Hachiya T, Suzuki S, Nishiyama R, Konno H, Muro H, Baba S (1993) Significance of hepatic vein reconstruction in hepatectomy. Surgery 114:59–64
12. Kaneoka Y, Yamaguchi A, Isogai M, Hori A (2000) Hepatic vein reconstruction by external iliac vein graft using vascular clips. World J Surg 24:377–382. doi:10.1007/s002689910060
13. Allema JH, Reinders ME, van Gulik TM, van Leeuwen DJ, de Wit LT, Verbeek PC, Gouma DJ (1994) Portal vein resection in patients undergoing pancreatoduodenectomy for carcinoma of the pancreatic head. Br J Surg 81:1642–1649. doi:10.1002/bjs.1800811126
14. Nakamura S, Hachiya T, Oonuki Y, Sakaguchi S, Konno H, Baba S (1993) A new technique for avoiding difficulty during reconstruction of the superior mesenteric vein. Surg Gynecol Obstet 177:521–523
15. Sakamoto Y, Yamamoto J, Saiura A, Koga R, Kokudo N, Kosuge T, Yamaguchi T, Muto T, Makuuchi M (2004) Reconstruction of hepatic or portal veins by use of newly customized great saphenous vein grafts. Langenbecks Arch Surg 389:110–113. doi:10.1007/s00423-003-0452-9
16. Urayama H, Katada S, Matsumoto I, Ishida F, Ohmura K, Watanabe Y, Muroki T (1993) Reconstruction of jugular and portal blood flows using remodeled great saphenous vein grafts. Surg Today 23:936–938. doi:10.1007/BF00311377
17. Doty DB, Baker WH (1976) Bypass of superior vena cava with spiral vein graft. Ann Thorac Surg 22:490–493
18. Kubota K, Makuuchi M, Sugawara Y, Midorikawa Y, Sakamoto Y, Takayama T, Harihara Y (1998) Reconstruction of the hepatic and portal veins using a patch graft from the right ovarian vein. Am J Surg 176:295–297. doi:10.1016/S0002-9610(98)00149-4
19. Heavrin BS, Wrenn K (2007) Ovarian vein thrombosis: a rare cause of abdominal pain outside the peripartum period. J Emerg Med 34:67–69. doi:10.1016/j.jemermed.2007.05.034
20. Schwartz JH, Sclafani SJ, Glass TA, Sewell PE (2008) Acute gonadal vein thrombosis secondary to terminal ileitis and thrombophilia. J Urol 180:1124. doi:10.1016/j.juro.2008.06.075
21. Hiromura T, Nishioka T, Nishioka S, Ikeda H, Tomita K (2004) Reflux in the left ovarian vein: analysis of MDCT findings in asymptomatic women. AJR Am J Roentgenol 183:1411–1415
22. Rebner M, Gross BH, Korobkin M, Ruiz J (1989) Appearance of right gonadal vein. J Comput Assist Tomogr 13:460–462. doi:10.1097/00004728-198905000-00017

23. Gokan T, Kushihashi T, Nobusawa H, Hashimoto T, Matsui S, Kitanosono T, Munechika H (2001) CT demonstration of dilated gonadal vein as a portosystemic shunt of mesenteric varices. J Comput Assist Tomogr 25:798–801. doi:10.1097/00004728-200109000-00021
24. Cancarini GC, Pola A, Pezzotti G, Tardanico R, Cozzoli A, Cunico SC (2002) Recovery of renal function after right nephrectomy, cavectomy and left renal vein ligation. J Nephrol 15:186–190
25. Leach SD, Lee JE, Charnsangavej C, Cleary KR, Lowy AM, Fenoglio CJ, Pisters PW, Evans DB (1998) Survival following pancreaticoduodenectomy with resection of the superior mesenteric-portal vein confluence for adenocarcinoma of the pancreatic head. Br J Surg 85:611–617. doi:10.1046/j.1365-2168.1998.00641.x
26. Lee S, Park K, Hwang S, Lee Y, Choi D, Kim K, Koh K, Han S, Choi K, Hwang K, Makuuchi M, Sugawara Y, Min P (2001) Congestion of right liver graft in living donor liver transplantation. Transplantation 71:812–814. doi:10.1097/00007890-200103270-00021
27. Ghobrial RM, Hsieh CB, Lerner S, Winters S, Nissen N, Dawson S, Amersi F, Chen P, Farmer D, Yersiz H, Busuttil RW (2001) Technical challenges of hepatic venous outflow reconstruction in right lobe adult living donor liver transplantation. Liver Transpl 7:551–555. doi:10.1053/jlts.2001.24910
28. Kubota T, Togo S, Sekido H, Shizawa R, Takeda K, Morioka D, Tanaka K, Endo I, Tanaka K, Shimada H (2004) Indication for hepatic vein reconstruction in living donor liver transplantation of right liver grafts. Transplant Proc 36:2263–2266. doi:10.1016/j.transproceed.2004.06.035
29. Sano K, Makuuchi M, Miki K, Maema A, Sugawara Y, Imamura H, Matsunami H, Takayama T (2002) Evaluation of hepatic venous congestion: proposed indication criteria for hepatic vein reconstruction. Ann Surg 236:241–247. doi:10.1097/00000658-200208000-00013

Synuclein-γ Is Closely Involved in Perineural Invasion and Distant Metastasis in Mouse Models and Is a Novel Prognostic Factor in Pancreatic Cancer

Taizo Hibi,[1,2,3] Taisuke Mori,[1] Mariko Fukuma,[1] Ken Yamazaki,[1] Akinori Hashiguchi,[1] Taketo Yamada,[1] Minoru Tanabe,[2] Koichi Aiura,[2] Takao Kawakami,[4] Atsushi Ogiwara,[5] Tomoo Kosuge,[3] Masaki Kitajima,[2] Yuko Kitagawa,[2] and Michiie Sakamoto[1]

Abstract

Purpose: Perineural invasion is associated with the high incidence of local recurrence and a dismal prognosis in pancreatic cancer. We previously reported a novel perineural invasion model and distinguished high– and low–perineural invasion groups in pancreatic cancer cell lines. This study aimed to elucidate the molecular mechanism of perineural invasion.

Experimental Design: To identify key biological markers involved in perineural invasion, differentially expressed molecules were investigated by proteomics and transcriptomics. Synuclein-γ emerged as the only up-regulated molecule in high–perineural invasion group by both analyses. The clinical significance and the biological property of synuclein-γ were examined in 62 resected cases of pancreatic cancer and mouse models.

Results: Synuclein-γ overexpression was observed in 38 (61%) cases and correlated with major invasive parameters, including perineural invasion and lymph node metastasis ($P < 0.05$). Multivariate analyses revealed synuclein-γ overexpression as the only independent predictor of diminished overall survival [hazard ratio, 3.4 (95% confidence interval, 1.51-7.51)] and the strongest negative indicator of disease-free survival [2.8 (1.26-6.02)]. In mouse perineural invasion and orthotopic transplantation models, stable synuclein-γ suppression by short hairpin RNA significantly reduced the incidence of perineural invasion ($P = 0.009$) and liver/lymph node metastasis ($P = 0.019$ and $P = 0.020$, respectively) compared with the control.

Conclusions: This is the first study to provide *in vivo* evidence that synuclein-γ is closely involved in perineural invasion/distant metastasis and is a significant prognostic factor in pancreatic cancer. Synuclein-γ may serve as a promising molecular target of early diagnosis and anticancer therapy.

Pancreatic ductal adenocarcinoma is currently the fourth leading cause of cancer-related death in Western countries (1). At the time of diagnosis, >80% of patients have locally advanced or metastatic disease and thus are not amenable for resection (2). Even in patients who underwent a histologically curative operation, long-term survival is rare, with the overall 5-year survival rates ranging from 10% to 25% (3, 4). Extensive local infiltration and early lymphatic and hematogenous spread likely contribute to the poor outcome of pancreatic cancer. Various criteria, such as tumor size, negative resection margins, histologic differentiation, lymph node metastasis, vascular involvement, and perineural invasion, have been proposed as prognostic indicators, but the results to date have been inconsistent (3–6). Of these, aggressive tumor extension into the perineural space even in the early stage of disease is a distinct mode of tumor spread in pancreatic cancer. High prevalence of local tumor recurrence even after curative resection is attributed to the residual tumor cells in the nerves of the remnant pancreas as well as the extrapancreatic nerve plexus that are undetected during the operation, leading to diminished survival. The striking incidence of perineural invasion in pancreatic cancer, ranging from 50% to 90%, underscores its importance (5, 6).

Recently, we established a mouse perineural invasion model and five human pancreatic cancer cell lines were divided into the high and the low-perineural invasion group (7). In the current study, proteomic analysis was used to compare protein expression profiles between these two groups to identify

Authors' Affiliations: Departments of [1]Pathology and [2]Surgery, Keio University School of Medicine; [3]Hepatobiliary and Pancreatic Surgery Division, National Cancer Center Hospital; [4]Clinical Proteome Center, Tokyo Medical University; and [5]Medical ProteoScope Co., Ltd., Tokyo, Japan

Received 11/11/08; revised 1/14/09; accepted 1/20/09; published OnlineFirst 4/7/09.

Grant support: The 21st Century Center of Excellence program and Cancer Research from the Ministry of Education, Science and Culture of Japan, and the 3rd Term Comprehensive 10-Year Strategy for Cancer Control from the Ministry of Health, Labor, and Welfare of Japan.

The costs of publication of this article were defrayed in part by the payment of page charges. This article must therefore be hereby marked *advertisement* in accordance with 18 U.S.C. Section 1734 solely to indicate this fact.

Note: Supplementary data for this article are available at Clinical Cancer Research Online (http://clincancerres.aacrjournals.org/).

Requests for reprints: Michiie Sakamoto, Department of Pathology, Keio University School of Medicine, 35 Shinanomachi, Shinjuku-ku, Tokyo 160-8582, Japan. Phone: 81-3-5363-3764; Fax: 81-3-3353-3290; E-mail: msakamot@sc.itc.keio.ac.jp.

doi:10.1158/1078-0432.CCR-08-2946

Translational Relevance

Aggressive tumor extension into the perineural space and adjacent lymph nodes even in the early stage of disease is a distinct mode of tumor spread in pancreatic cancer; however, its molecular mechanism remains unclear. This is the first study describing *in vivo* evidence that synuclein-γ is closely involved in perineural invasion/distant metastasis using mouse models and is a significant predictor of survival in resected cases of pancreatic cancer. Because 33% of patients with stage I disease in our series showed synuclein-γ overexpression, synuclein-γ may become an indicator for early diagnosis. To optimize the magnitude of pancreatic surgery, the extent of neural plexus resection and lymph node dissection may be determined according to the preoperative synuclein-γ status. Stratification of resected cases by synuclein-γ status is also worth considering to customize postoperative multidisciplinary approach. Synuclein-γ may well serve as a novel molecular target of anticancer therapy of this devastating disease.

differentially expressed proteins that may play a role in perineural invasion, reflecting the more aggressive tumor phenotype. Among the overexpressed proteins that emerged from quantitative proteomics, we selected synuclein-γ (SNCG) for further investigation because its corresponding mRNA was also up-regulated in the high-perineural invasion group (7). To clarify the clinical significance of SNCG expression in pancreatic cancer, the medical records of resected cases were retrospectively reviewed, focusing on the correlations with clinicopathologic factors as well as prognosis. The effect of stable SNCG suppression in the high-perineural invasion group was evaluated *in vivo* using mouse perineural invasion and orthotopic transplantation models.

Materials and Methods

Cell lines and laboratory animals. Five human pancreatic cancer cell lines, Capan-1, Capan-2, AsPC-1, Panc-1, and HPAF-II, were obtained from the American Type Culture Collection. Eight- to 12-wk-old, nonobese diabetes/severe combined immunodeficient mice were used. All studies were conducted in accordance with the U.S. Public Health Service Policy on Humane Care and Use of Laboratory Animals, NIH.

Perineural invasion model and orthotopic (pancreas) transplantation model in mice. The human pancreatic cancer cell lines were harvested from confluent cultures, washed twice with PBS, and resuspended in a serum-free RPMI 1640. For the perineural invasion model, mice were anesthetized, and 6 to 7 × 10^6 viable tumor cells in 100 μL of cell suspension were injected s.c. on the midline of their backs at two sites using an inoculator fitted with a 23-gauge needle. Six to 8 wks after injection, the tumor was resected with a 5-mm margin of the neighboring skin to examine the degree of perineural invasion to the mouse s.c. nerves (7).

For the orthotopic transplantation model, the mice were anesthetized and the distal pancreas exteriorized as described previously (8), and ~ 10^6 viable tumor cells in 10 μL of cell suspension were injected into the pancreas using an inoculator with a 27-gauge needle. The pancreas was relocated into the abdominal cavity, and the peritoneum and skin were closed with a surgical stapler. Five to 6 wks after injection, the mice were sacrificed, and the pancreas, stomach, duodenum, liver, lymph nodes, lungs, and other organs of suspected tumor involvement or metastasis were harvested.

Proteomic analysis. Tumor cells of the human pancreatic cancer cell lines were homogenized in PBS supplemented with a protease inhibitor cocktail (Roche Diagnosis) and fractionated by ultracentrifugation (52,000 × *g*; 4°C; 20 mins). The resulting pellet, containing plasma membranes from the cells, was solubilized in PBS containing 5% SDS with continuous ultrasonication. The resulting solution was taken as the insoluble fraction, whereas the supernatant from the ultracentrifugation, containing mainly cytosolic proteins, was taken as the soluble fraction. An aliquot (50 μg of protein) from each fraction was subjected to SDS-PAGE on a 12.5% polyacrylamide gel 1 mm thick. SDS-PAGE was carried out until the bromophenol blue marker passed the boundary between the stacking and separation gels so that almost all proteins were condensed in a small area between the gel boundary and the blue marker. This small gel area was then excised from the gel slab, and the gel slice, including proteins, was subjected to in-gel tryptic digestion (9).

The resulting small peptide mixture (1 μg) was analyzed using a liquid chromatography-tandem mass spectrometry (MS/MS) system in a fully automated manner (10, 11). A reversed-phase peptide separation was done on a C18 capillary column (Michrom Bioresources) at a flow rate of 1 μL/min. The liquid chromatography effluent was directly interfaced with an electrospray ionization source in a positive ion mode modified on a Finnigan LTQ linear ion trap mass spectrometer (Thermo Fisher Scientific; ref. 12). The electrospray ionization-MS/MS operation and continuous data acquisition of full MS scan and subsequent three MS/MS scans were carried out on an Xcalibur system controller (Thermo Fisher Scientific).

All full MS data were investigated using an i-OPAL differential liquid chromatography -MS data analysis system (i-OPAL algorithm; patent WO2004/090526 AI). Firstly, the signal intensity of the full MS scan was normalized so that the total signal intensity of each data became the same value. Several standard signals, derived either from the coanalyzed egg white lysozyme or from sample intrinsic common proteins, were selected as i-OPAL alignment markers. The i-OPAL alignment program was used to align the nonlinearly fluctuating liquid chromatography retention time axis of all liquid chromatography -MS data to finally generate a single combined liquid chromatography -MS data for the soluble fraction and the insoluble fraction, respectively. A *t* test was applied for each peak signal in the final combined liquid chromatography -MS data to select candidate marker signals whose intensity differed significantly within a cell type. Statistical analysis was done using Spotfire DecisionSite software package.

All MS/MS data were investigated using Mascot search program (Matrix Science;[6] ref. 13) against the *Homo sapiens* (human) subset of the Swiss-Prot and the RefSeq protein sequence databases. The database searches were done allowing for fixed modification of cysteine residue (*S*-carbamidomethylation, +57.0 Da) and variable modification of methionine residue (oxidation, +16.0 Da), peptide mass tolerance at ±2.0 Da, and product ion tolerance at ±0.8 *m/z* unit.

The proteomic analysis was done in duplicate for each cell line. An liquid chromatography -MS/MS measurement generated a single two-dimensional signal profile and >10,000 product ion spectra acquired by dissociation of peptide ions. To identify proteins involved in perineural invasion, we compared the signal profiles between the high- and low-perineural invasion cell line groups. We filtered all the peaks detected in the signal profiles according to the following conditions: (*a*) the liquid chromatography retention time between 5 and 75 mins, (*b*) the *m/z* value of ≤1,500, and (*c*) the *P* value of the Student's *t* test between the high-perineural invasion and the low-perineural invasion groups <0.001.

Patients and resected specimens. We reviewed the medical records of 67 consecutive patients who underwent resection with curative intent for invasive ductal pancreatic adenocarcinoma from 1995 through 2004 at Keio University Hospital, Tokyo, Japan. Five patients who suffered

[6] http://www.matrixscience.com

in-hospital death were excluded, and a total of 62 patients with available follow-up data comprised the subjects of this retrospective study. Two pathologists examined all resected specimens to confirm the histopathologic diagnosis of pancreatic adenocarcinoma according to the Japan Pancreas Society Classification (14). The tumor node metastasis system of the Unio Internationale Contra Cancrum (UICC) was used for staging (15). This study was conducted under the approval of the Ethics Committee of Keio University School of Medicine (approval 16-34-1).

The definition and the degree of perineural invasion were determined as described previously (7). Other pathologic factors are summarized in Table 1. Outcome measures included disease-free and overall survival. The diagnosis of tumor recurrence or metastasis was based on radiological findings. Survival time was calculated as the period from the date of surgery until death or the most recent clinic visit.

Immunologic analysis and quantitative reverse transcriptase-PCR. A goat anti-SNCG polyclonal antibody (Santa Cruz Biotechnology) was utilized. Immunohistochemical staining was evaluated by two independent observers who were not aware of the clinicopathologic data of the corresponding tumor in the surgical cases and the SNCG suppression status in the mouse models. Positive control samples were described previously (16). In the surgical specimens, peripheral nerves also served as an internal control. SNCG positive was defined as ≥10% staining of the tumor. Immunofluorescence, Western blotting, and quantitative reverse transcriptase-PCR analysis were described previously (7). In quantitative reverse transcriptase-PCR, the primer set was 5′-AACACTGTGGCCACCAAGAC-3′ (forward) and 5′-GATGGCCTCAAGTCCTCCTT-3′ (reverse), which corresponds to the coding region of the SNCG transcript.

Vector construction and retroviral infection. Vector construction and production of recombinant retroviruses were described previously (17, 18). To generate two short hairpin RNA (shRNA) expression vectors for SNCG, that is, pSI-CMSCVpuro-H1R-SNCGshRNA-A and pSI-CMSCVpuro-H1R-SNCGshRNA-B, the targeted sequences were 5′-TGGAGGAGGCGGAGAACAT-3′ and 5′-CCGAGAAGACCAAGGAGCA-3′, respectively. For the control (nontargeting sequence) shRNA expression vector, namely, pSI-CMSCVpuro-H1R-Control, the sequence was 5′-TAAGGCTATGAAGAGATAC-3′. Two stable SNCG-suppressed Capan-1 cells and the Control Capan-1 cells were designated sh-A, sh-B, and sh-Control, respectively.

Statistical analysis. Unless otherwise indicated, all data were determined from three independent experiments, with each of them done in triplicate. The data are expressed as mean values ± SD. The mRNA levels of SNCG in each cell line were compared by Student's *t* test (two tailed). The χ^2 test or Fisher's exact probability test were used when appropriate to determine the correlations between clinicopathologic variables and SNCG expression. Survival rates were calculated with the Kaplan-Meier method, and the log-rank test was applied to compare survival between different groups. Significant prognostic factors revealed by the log-rank tests were included in the multivariate analysis using the Cox proportional hazard model. Statistical significance was defined as $P < 0.05$. All statistical analyses were done using SPSS statistical software (SPSS, Inc.).

Table 1. Correlations between SNCG expression and histopathologic factors

Variables	SNCG expression, *n* (%)		*P*
	Negative, *n* = 24	Positive, *n* = 38	
Tumor size, mm			0.014
≤20	11 (46)	6 (16)	
>20	13 (54)	32 (84)	
Serosal invasion			0.081
Absent	22 (92)	28 (74)	
Present	2 (8)	10 (26)	
Retroperitoneal extension			0.84
Absent	12 (50)	18 (47)	
Present	12 (50)	20 (53)	
Portal vein involvement			0.97
Absent	14 (58)	22 (58)	
Present	10 (42)	16 (42)	
Lymph node metastasis			0.009
Negative	12 (50)	7 (18)	
Positive	12 (50)	31 (82)	
Resection status			0.15
R0	19 (79)	24 (63)	
R1	5 (21)	14 (37)	
UICC stage			0.009
IA/IB/IIA	12 (50)	7 (18)	
IIB/III/IV	12 (50)	31 (82)	
Histologic differentiation			0.069
Well	11 (46)	9 (24)	
Moderate, poor	13 (54)	29 (76)	
Lymphatic invasion			0.091
0-1	16 (67)	17 (45)	
2-3	8 (33)	21 (55)	
Vascular invasion			0.027
0-1	17 (71)	16 (42)	
2-3	7 (29)	22 (58)	
Perineural invasion			0.033
0-1	12 (50)	9 (24)	
2-3	12 (50)	29 (76)	

Results

Proteomic analysis. We obtained 214 peaks in which 171 were up-regulated and 43 were down-regulated. A two-way hierarchical clustering algorithm successfully distinguished between the high-perineural invasion and the low-perineural invasion groups (Fig. 1A). Peptide identifications to the product ion spectra were screened according to a Mascot scoring value as the ion score representing the significance of identification. The peptide identification of the highest ion score with >30 was adopted per peak. Of the 214 peaks, 211 were linked to specific peptide identification, whereas the remaining 3 peaks were given with no identification under the present conditions. Database entry names from Swiss-Prot[7] or RefSeq[8] as the source of the peptide identifications are shown in Fig. 1A.

SNCG expression in human pancreatic cancer cell lines. Among the proteins listed in Fig. 1A, SNCG was selected for further investigation because its corresponding RNA level also showed significant up-regulation in the previous microarray analysis comparing the high- and low-perineural invasion groups (7). Quantitative reverse transcriptase-PCR was used for total RNA samples isolated from five pancreatic cancer cell lines to analyze the SNCG mRNA levels. The relative expression level of SNCG was significantly higher in the high-perineural invasion group compared with the low-perineural invasion group ($P = 0.0001$; Fig. 1B). Protein overexpression of SNCG in Capan-1 and Capan-2 was subsequently confirmed by Western blotting (Fig. 1B).

The immunohistochemical properties of cell lines for SNCG were evaluated in the tumors of the mouse perineural invasion model. SNCG staining was strongly positive (>90% of all tumor

[7] http://br.expasy.org/sprot/
[8] http://www.ncbi.nlm.nih.gov/RefSeq/

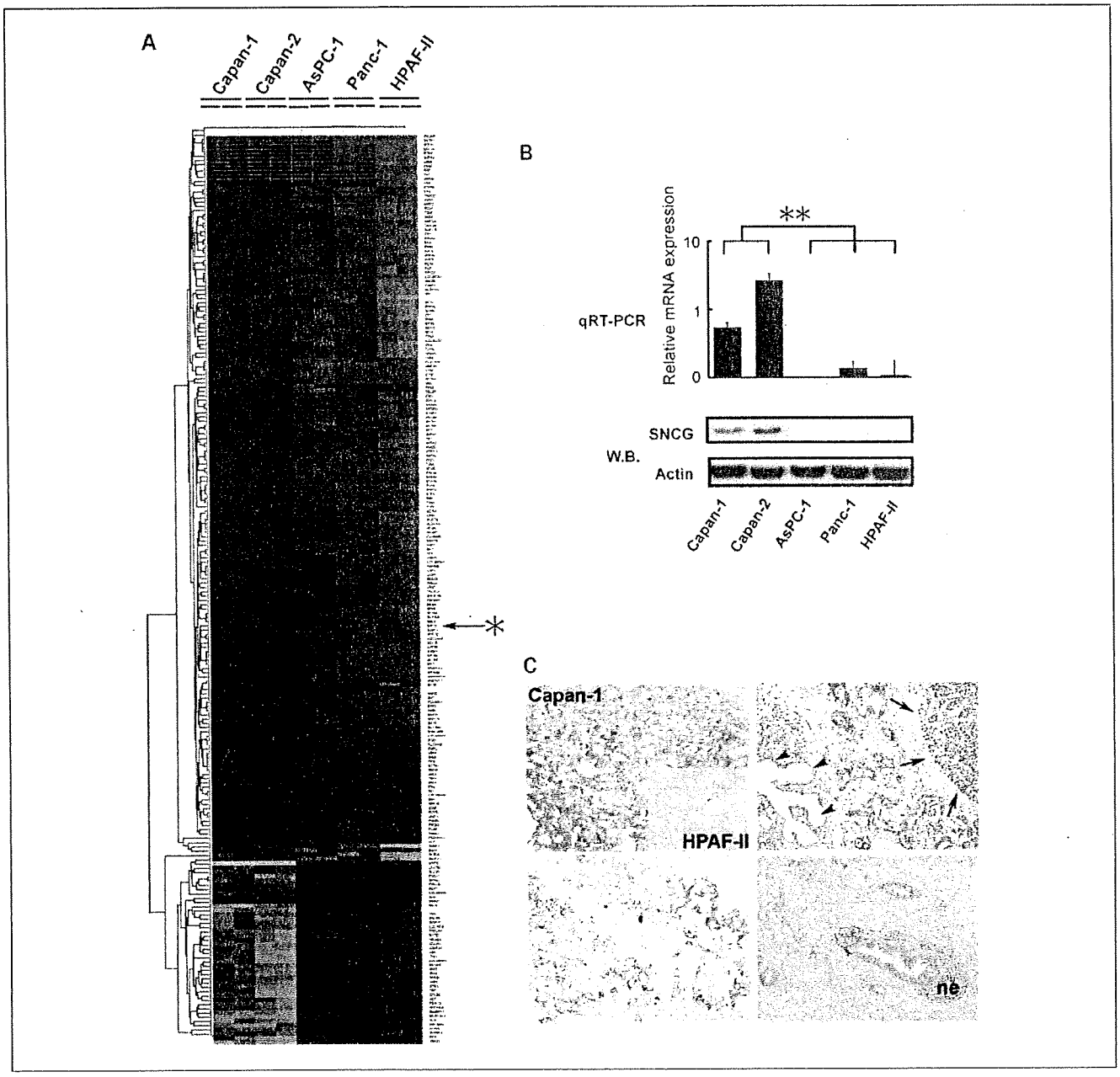

Fig. 1. *A*, proteomic analysis. Two-way hierarchical clustering algorithm successfully differentiated 214 peptide ion signals by peak intensity between high – perineural invasion (Capan-1 and Capan-2) and low – perineural invasion (AsPC-1, Panc-1, and HPAF-II) groups. Color patch, the peak intensity of the corresponding peptide in each cell line as a continuum of relative expression levels from lowest (*green*) to highest (*bright red*). *, SNCG. *B*, quantitative reverse transcriptase-PCR analysis and Western blotting. W.B., Western blotting. of SNCG in five human pancreatic cancer cell lines. SNCG mRNA and protein expression levels were significantly higher in the high – perineural invasion group compared with the low – perineural invasion group. **, $P = 0.0001$. *C, top left plate*, immunohistochemical properties of cell lines. Capan-1 showed strongly positive staining for SNCG compared with consistently negative HPAF-II (*inset*). *Top right/bottom left/bottom right plates*, in surgically resected specimens, the pancreatic cancer cells showed heterogeneous staining for SNCG, whereas the normal pancreas (*arrowheads*, pancreatic ducts; *arrows*, acinar cells) were mostly negative. ne, nerves.

cells) in the high – perineural invasion group, whereas the low – perineural invasion group was universally negative under the same condition (Fig. 1C). SNCG localization was observed mainly in the cytoplasm with focal nuclear staining.

Clinical significance of SNCG overexpression in resected cases of pancreatic cancer. The median age of the 62 patients (40 men and 22 women) meeting our eligibility criteria was 67 years (range, 45-83 years). Two tumors were categorized as UICC stage IA, 4 as stage IB, 13 as stage IIA, 34 as stage IIB, 1 as stage III, and 8 as stage IV. All stage IV cases were nodal metastasis beyond the regional lymph node station, including the para-aorta ($n = 6$), the distal mesenteric ($n = 1$), and the lesser curvature of the stomach ($n = 1$). Figure 1C exemplifies the representative SNCG staining properties of the resected specimens. The pancreatic ducts and the acinar cells of the nontumorous pancreas showed mostly negative to faint